Possible link between irrigation in the U.S. High Plains and increased summer streamflow in the Midwest

M. Deniz Kustu,[1] Ying Fan,[1] and Matthew Rodell[2]

Received 29 September 2010; revised 8 December 2010; accepted 6 January 2011; published 19 March 2011.

[1] We have previously presented evidence that higher rates of evapotranspiration (ET) associated with irrigation in the U.S. High Plains has likely caused an increased downwind precipitation (*P*). July *P* over the Midwest increased by 20%–30% from the preirrigation period (1900–1950) to the postirrigation (1950–2000) period. In this study, we test the hypothesis that the increased July *P* has had hydrologic consequences, possibly increasing groundwater storage and streamflow. Seasonal analyses of hydrologic variables over Illinois suggest that the water table and streamflow response lags $P - \mathrm{ET}$ by 1–2 months, indicating August and September as the months when the increased July *P* may be detected. We analyzed long-term observations of water table depth at 10 wells in Illinois and streamflow at 46 gauges in Illinois-Ohio basins. The Mann-Kendal test for trends suggests field significant increases in groundwater storage and streamflow in August–September over the period of irrigation expansion. Examination of soil moisture response to present-day above-normal July *P* suggests that the increased July *P* can reach the water table in normal to wet years. Mann-Kendall tests suggest that there has been no change in pan evaporation and atmospheric vapor pressure deficit. This implies that soil water availability is the driver of changes in ET, and the increased *P* may have possibly increased ET. Other studies in the literature give further evidence of increased ET due to increased *P*. By ruling out a reduction in ET, we suggest that the observed increase in groundwater storage and streamflow in the Midwest is linked to the increased July precipitation attributed to High Plains irrigation. We note that the increases in late summer streamflow are rather small when placed in the context of seasonal dynamics, but they are conceptually important in that they point to a different cause of change.

Citation: Kustu, M. D., Y. Fan, and M. Rodell (2011), Possible link between irrigation in the U.S. High Plains and increased summer streamflow in the Midwest, *Water Resour. Res., 47*, W03522, doi:10.1029/2010WR010046.

1. Introduction

[2] Groundwater pumping for irrigation in the U.S. High Plains began to accelerate in the 1940s (Figure 1a), and by the mid-1980s, groundwater levels had declined by >30 m over much of the High Plains (Figure 1b) [*McGuire*, 2009]. The decades-long and regional-scale water transfer, from the groundwater reservoir to the soil moisture reservoir in the warm season, has likely influenced the region's hydrology and climate. Moreover, this influence may not have been confined to the High Plains itself but may have propagated downwind through the atmospheric vapor transport pathways and down gradient through the river and groundwater pathways. We hypothesize the following: first, the large groundwater decline has led to reduced streamflow in the High Plains region wide, particularly where groundwater is a source for streamflow; second, because irrigation drastically increases warm season evapotranspiration (ET), it has increased vapor export and possibly downwind precipitation (*P*); third, such increased downwind *P* has altered the land hydrology over the receiving region, far away from the High Plains where the change originated. Figure 1c schematically illustrates these hypotheses: (1) reduced streamflow in the High Plains, (2) increased downwind *P*, and (3) increased downwind ET and streamflow.

[3] In an earlier paper [*Kustu et al.*, 2010], we tested the first hypothesis. That groundwater pumping in the High Plains reduced streamflow was not a new idea; there had been many reports in the literature on the subject (see detailed review by *Kustu et al.* [2010]), but they focused on specific areas and applied different methods of analysis, leaving large spatial gaps and making a regional comparison and synthesis difficult. For example, strong climatic and hydrologic gradients from northern to southern High Plains are well documented. In the north (e.g., Nebraska), the cooler and moister climate, the sandy soil and river beds, and the naturally high water table point to groundwater as a main source for streamflow and that changes in the former can directly influence the latter. In the south (e.g., Texas), the warm and dry climate, the dominance of summer thunderstorms and surface runoff, and the naturally deep water

[1]Department of Earth and Planetary Sciences, Rutgers, State University of New Jersey, New Brunswick, New Jersey, USA.
[2]Hydrological Sciences Branch, NASA Goddard Space Flight Center, Greenbelt, Maryland, USA.

Copyright 2011 by the American Geophysical Union.
0043-1397/11/2010WR010046

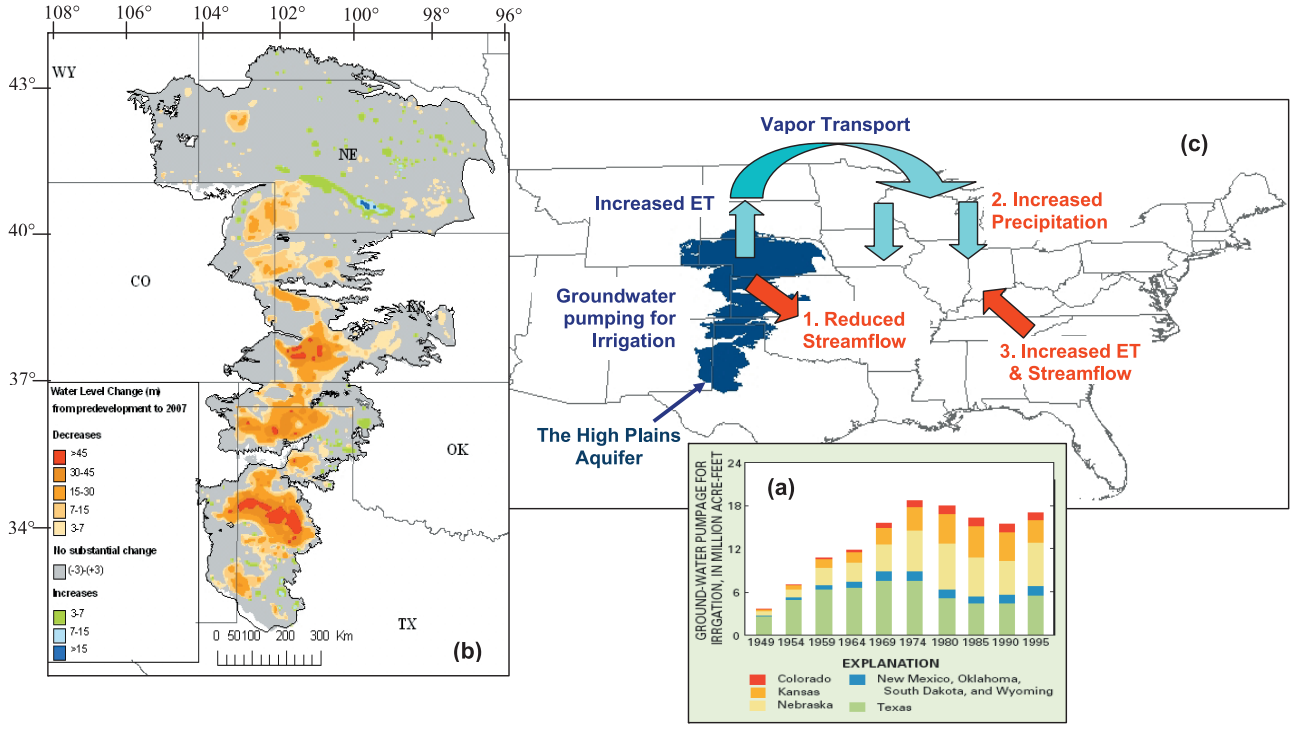

Figure 1. (a) Volume of groundwater pumped for irrigation from the U.S. High Plains aquifer for selected years [from *McGuire et al.*, 2003], (b) the resulting water table decline [from *McGuire et al.*, 2009], and (c) possible effects of High Plains irrigation on the regional water cycle.

table indicate that the water table may lie below local river beds; hence, pumping may have little effect on local streamflow (but it may affect regional streams fed by regional groundwater convergence further down gradient). To achieve this regional synthesis, we analyzed the entire groundwater and streamflow records of the U.S. Geologic Survey (USGS). Our results filled large spatial gaps between previously studied areas and suggest that indeed, decreases in annual and dry season streamflow and increases in the frequency of low-flows are more pronounced in the northwestern part of the High Plains.

[4] In our second study [*DeAngelis et al.*, 2010], we tested the second hypothesis that irrigation in the High Plains, through increased ET and vapor export, may influence downwind precipitation. The idea that irrigation can affect rainfall is not new either (see detailed review by *DeAngelis et al.* [2010]), but earlier studies focused on local *P* recycling and were based on short-term observations or model experiments. It is now well recognized that land surface wetness has a large impact on downwind precipitation [e.g., *Dominguez et al.*, 2009; *van der Ent et al.*, 2010], and a recent global modeling study [*Puma and Cook*, 2010] reports larger downwind than local increases in precipitation due to irrigation. In the United States, it is well understood that the strong winds of the Great Plains Low Level Jet [*Weaver et al.*, 2009] (see wind vectors in Figure 2a), peaking in the warm season, connect the High Plains (region 1 in Figure 2a) to its downwind regions to the northeast. Meanwhile, hundreds of station precipitation records exist in the central United States, dating back to at least the early 1930s. A study based on these long-term precipitation observations with an emphasis on downwind climatic impacts had been lacking. To fill in this knowledge gap, we analyzed 865 long-term station records, over and downwind of the High Plains (the three regions in Figure 2a), for signals of change. The observations, combined with a Lagrangian vapor tracking analysis to trace the fate of the High Plains ET, revealed evidence that irrigation in the High Plains has led to increased downwind precipitation, particularly over the Midwest (region 3 in Figure 2a) in the month of July, the peak month of irrigation and the peak month of wind speed in the Great Plains Low Level Jet [*Weaver et al.*, 2009].

[5] In this paper, we test our third hypothesis that the irrigation-enhanced July precipitation over the Midwest has had hydrologic consequences. Precipitation is a key driver of land hydrology, and changes in *P* will propagate through the various hydrologic pathways: canopy interception, surface runoff, infiltration, soil and plant ET, water table recharge, and groundwater discharge into streams. The noticeable increase in July *P* from the first to the second half of the century (Figure 2b) likely manifested itself in one or more of these hydrologic variables. In this paper, we analyze available observations of these hydrologic variables to search for signals of change that may be attributable to the increased July precipitation.

[6] In section 2, we discuss the dominant hydrologic pathways in the region and the associated time scales whereby precipitation propagates through land hydrology. In section 3, we analyze long-term water table, streamflow, soil moisture, air temperature, and pan evaporation time series. In section 4, we discuss the implications of the work and future research to improve our understanding of hydrologic-climatic interactions in the context of climate variability and change and land use or water use changes.

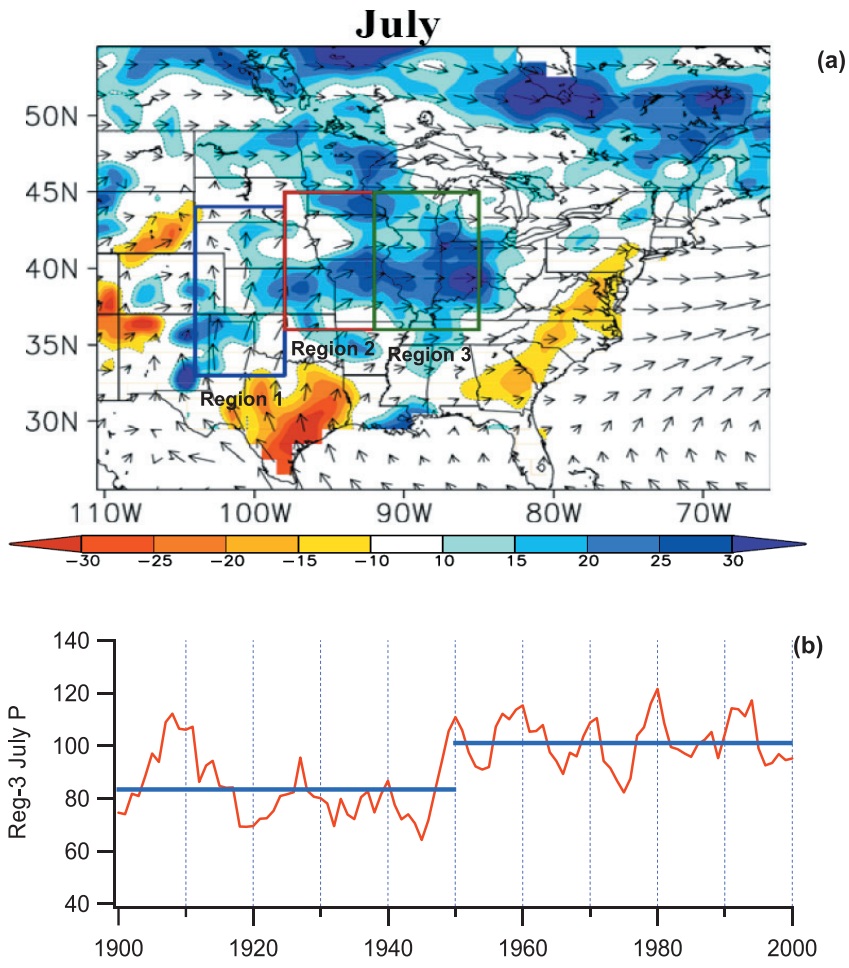

Figure 2. (a) Spatial pattern of July precipitation change (%) between the periods of 1900–1950 and 1950–2000 and mean July 850 mbar wind fields (m/s) over 1979–2001, obtained from North America Regional Reanalysis (for details, see *DeAngelis et al.* [2010]). (b) Time series of July precipitation (mm) averaged over 316 station records within region 3 (green box in Figure 2a), shown as a 5 year moving average and with the means (blue) of the first and second halves of the century (84 and 102 mm, respectively, tested statistically significant in the work of *DeAngelis et al.* [2010]). The green box is the area of focus in this study.

2. Hydrologic Features of the Study Area

[7] The study area is centered over the states of Illinois and Indiana (Figure 2a, green box), where July precipitation increased by 10%–30% from the first half to the second half of the twentieth century. The change occurred near the middle of the century (Figure 2b), after which the means and lows all increased and extreme dry periods have been absent. The questions are, how does such a change in July P (hereafter referred to as July ΔP) propagate through land hydrology, and can we detect its signal in historically observed hydrologic variables such as water table depth and streamflow?

[8] As precipitation increases, the vegetation and the near-surface soils are the first to sense it, and if ET is water limited, ΔP will likely engender increased ET, leaving no trace in groundwater and streamflow (historically observed). However, if ET is energy limited, then ΔP may infiltrate deeper and recharge the groundwater, leaving a signature in groundwater and river flow. It may also take the route of increased surface runoff if ΔP is in the form of higher storm intensity.

[9] To explore the possible partition of ΔP into increased ET (not observed) versus groundwater storage and streamflow (observed), we examine the seasonality of land hydrology in the region. Illinois has one of the best hydrologic monitoring networks in the world, including soil moisture beginning in 1981 [*Hollinger and Isard*, 1994] and shallow water table in the late 1950s (Illinois State Water Survey (ISWS)). Although they began after the initial irrigation expansion, the water table records cover a good portion of the period. In addition, soil moisture and water table observations provide essential insight into the cascading of P signals through the hydrologic stores and the associated time scales.

[10] Figure 3a plots the seasonal cycle of observed P, estimated ET, and observed streamflow (the fluxes), and Figure 3b plots the seasonal cycle of the observed top 2 m soil moisture (SM) and water table depth (WTD) (the

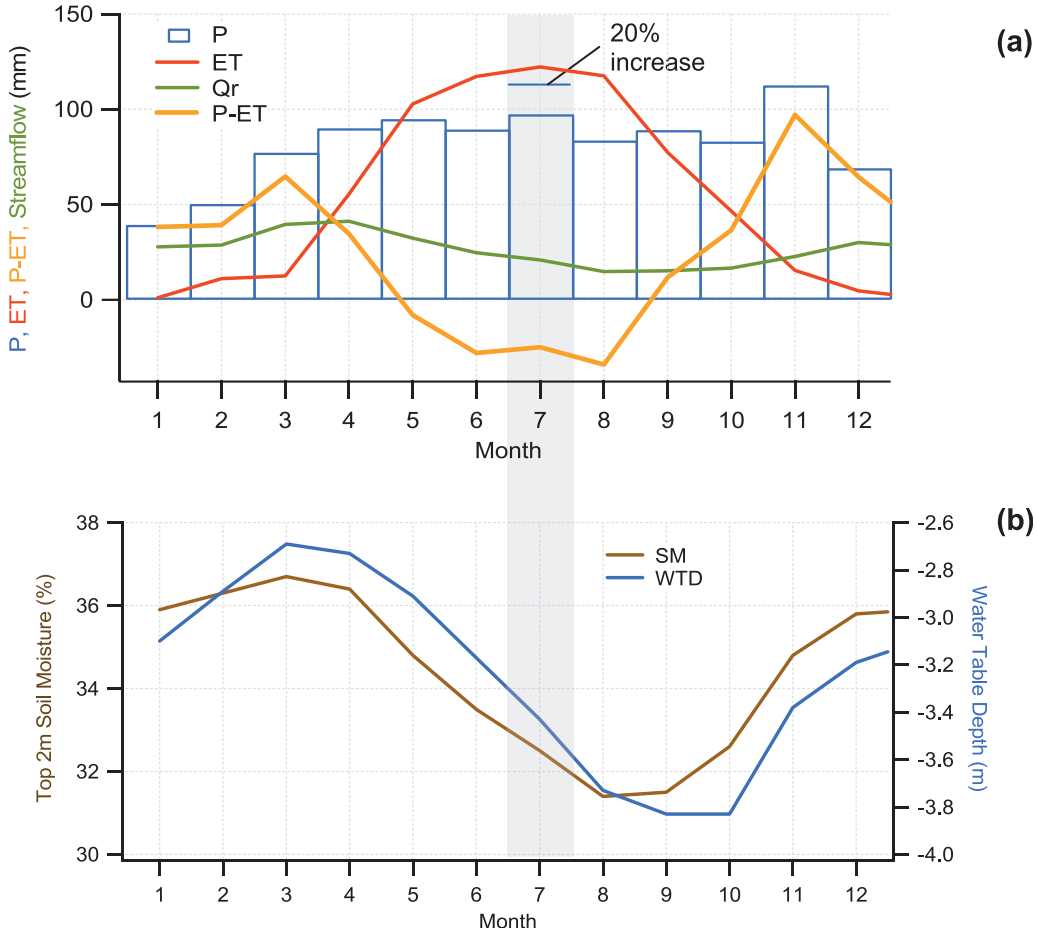

Figure 3. Seasonal cycle in (a) hydrologic fluxes: precipitation (P), evapotranspiration (ET), soil water surplus (P − ET), and streamflow (Q_r). (b) Hydrologic states: soil moisture (SM) and water table depth (WTD) (data are from *Eltahir and Yeh* [1999]).

states), averaged over the state of Illinois and the period of 1983–1995. The data in Figure 3 are directly taken from the work by *Eltahir and Yeh* [1999], which is a seminal study on the hydrologic linkages in the region, where the ET is the mean of two independent estimates, one based on atmospheric vapor convergence and the other on soil water budget analysis [*Yeh et al.*, 1998]. We note the following.

[11] First, ET flux, with its large seasonal swings, dominates the seasonal dynamics, exceeding P in May through August. In July, P accounts for 80% of ET, suggesting a net soil water deficit (P − ET < 0). Long-term mean July pan evaporation in central Illinois is 227 mm (as shown later in Figure 10b and Table 6), suggesting that the 122 mm ET here is below potential and that a July ΔP of ~20% may directly translate into increased July ET. However, if higher storm intensity accounts for ΔP, it would lead to increased infiltration excess surface runoff, leaving a signature in streamflow. Since surface runoff responds to rainfall quickly, the signature in streamflow would be found in the same month (July). If ΔP represents longer periods of rainfall, it would increase infiltration into the soil.

[12] Second, the top 2 m soil moisture closely follows the P-ET cycle, with the best correlation obtained at the 1 month lag (Figure 4a). That is, the top 2 m soil moisture as a whole responds to climate forcing 1 month later, although the shallow soils may respond in the same month. Therefore, the signal of ΔP is likely found in July (at shallow depths) and August (at deeper depths) in the soil moisture records.

[13] Third, the water table cycle closely follows the soil moisture cycle, with the best correlation obtained at the 1 month lag (Figure 4b). That is, the groundwater on average is recharged 1 month after the soil moisture is replenished. This suggests that the signal of ΔP is likely found in the groundwater records (if at all) in August and September.

[14] Fourth, groundwater fluctuations are closely linked to streamflow. The streamflow seasonal cycle is mostly in phase (no lag) with that of the water table depth (Figure 4c). *Eltahir and Yeh* [1999] estimated that surface runoff explains <10% of streamflow variations and accounts for <25% of streamflow, leaving groundwater as the main source and driver of monthly and seasonal dynamics. This suggests that the July ΔP signal would find expressions (if at all) in August and September streamflow.

[15] The above analysis is summarized in Figure 4d with the expected lag times of the relevant hydrologic variables indicated. The above discussion helps us focus our

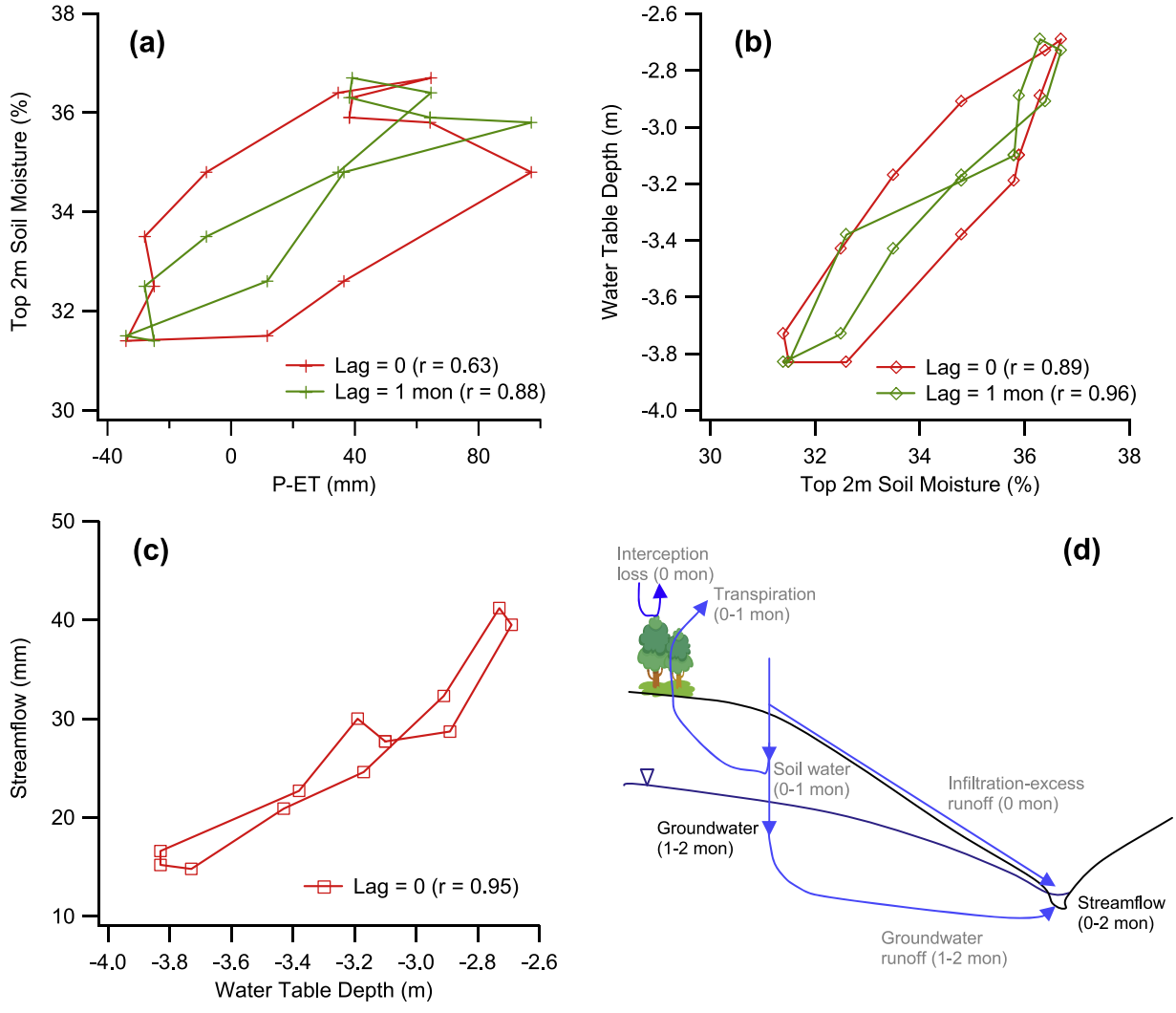

Figure 4. Phase relations between (a) soil moisture and $P - \mathrm{ET}$, (b) water table depth and soil moisture, and (c) streamflow and water table depth, with the Pearson correlation coefficient (r) given for the different lags. (d) Summary of the lag time of response of the hydrologic variables, where black lettering indicates variables that are observed over the period of interest (1940–1980).

subsequent analysis on relevant hydrologic variables and at relevant time scales.

3. Signals of Increased July *P* in the Observed Hydrologic Variables

[16] Figure 5 gives the mean region 3 (Figure 2a) precipitation time series (shown as a 5 year moving average to highlight long-term variabilities) for May–September based on 316 station monthly data from the National Climate Data Center (NCDC, http://www.ncdc.noaa.gov/oa/ncdc.html). They are shown here because the signal of May and June P may be present in July and August water table level and streamflow. Over the period of irrigation expansion (1940–1980, shaded gray in Figure 5), there is a slight decline in May and June, a step-like increase midcentury in July, a rise in late 1970s in August, and no apparent trend in September. Of the hydrologic variables in Figure 4d, only the groundwater level and streamflow are observed over the period of interest (1940–1980), and we start our analysis with these observations.

3.1. Changes in Water Table Depth

[17] Water table observations, dating back to the 1950s, are obtained from USGS at one site (all others began in the late 1980s) at ~10 day steps and at nine sites from the ISWS Water and Atmosphere Resource Monitoring network (WARM, http://www.isws.illinois.edu/warm/sgwdata/wells.aspx) at monthly steps. All these long-term observations are in the state of Illinois; no historic groundwater data could be found for Indiana, where the largest July ΔP was observed (Figure 2a). The well locations are shown in Figure 6a (orange and green), with site information given in Table 1 (see the wells with early data; the rest have shorter records and are used for later analyses). Monthly water table depths at these 10 sites are plotted in Figure 7 for July–September.

[18] In July, more sites showed an upward trend despite the flat or downward trend in May and June P. In August and September, the upward trend is more apparent. Table 2 gives the result of the statistical test for water table trends in July to September over the period of 1940–1980,

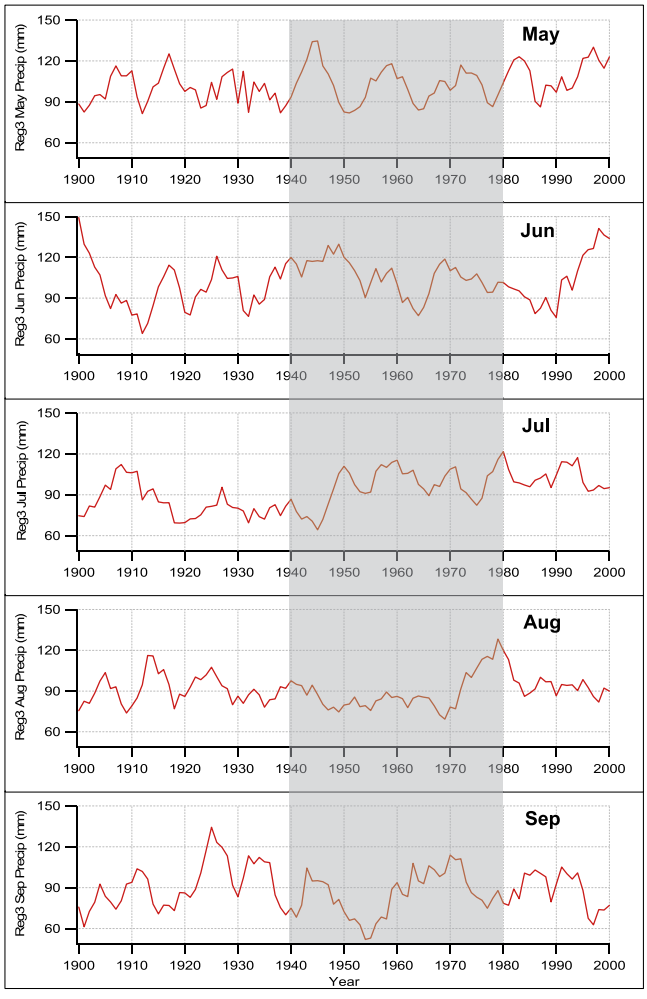

Figure 5. Region 3 mean monthly rainfall (5 year moving average) for May through September based on 316 station records, with the irrigation development period (1940–1980) shaded gray.

using the nonparametric Mann-Kendall test [*Mann*, 1945; *Kendall*, 1975]. Eight of the 10 sites show a rising trend in the July water table, but it is statistically significant (at 5% level, or $p < 0.05$, shown in bold) at only two sites, and one site (W191) has a significant falling trend. In August and September, the number of sites with significant rising trends increased, consistent with our expectation that if the signal of ΔP is to be detected in the groundwater, it would be in August and September. The decreasing trends at W61 (August) and W191 (August–September) are unexplained.

[19] We also evaluate the field significance of the trend test results, which is necessary when assessing regional trends at multiple sites [e.g., *Livezey and Chen*, 1983; *Lettenmaier et al.*, 1994; *Douglas et al.*, 2000; *Yue and Wang*, 2002; *Renard et al.*, 2008; and *Khaliq et al.*, 2009]. Field significance (α) is the combined significance of N tests; if the percentage of significant results is greater than α, then the results are said to be field significant. Two methods can be used. If the sites are spatially independent, α follows the binomial distribution. The wells used for the trend analysis (orange and green in Figure 6a) are isolated from one another by several streams, and we consider them hydrologically independent (e.g., land use change or pumping near one well will not affect another). The binomial test [*Livezey and Chen*, 1983] indicates that the water table trends are field significant at the 5% level in August and September but not in July (they might have occurred by chance). If the multiple sites are not independent, then the regional Kendall's S test [*Douglas et al.*, 2000] is appropriate, results of which suggest that the water table trends are not field significant in any of the months.

3.2. Changes in Streamflow

[20] Streamflow records were obtained from the USGS National Water Information System (NWIS) database (http://nwis.waterdata.usgs.gov/nwis/sw) for a total of 1428 gauges in the Ohio River basin and 343 in the Illinois River basin. We selected 46 gauges (24 in the Ohio basin and 22 in the Illinois basin) for this study according to the following criteria. First, they are located in areas where more than 10% of July ΔP is detected (see Figure 2a). Second, their records cover at least 30 years, starting no later than 1941 and ending no earlier than 1970. Third, the streams are not affected by reservoirs which cause significant changes in streamflow, especially during summer months, making attributions of change difficult [*Yang et al.*, 2004; *Haddeland et al.*, 2007]; however, those gauges where regulation began after 1970 are retained with the data after the changes removed. Fourth, these streams do not drain into one another, so each gauge represents an independent measurement; if one drains into another, the larger basin is retained. Figure 6b gives the location of the 46 gauges selected (yellow), as well as all the gauges considered (pink) and the dams (light blue) that rendered many stations unusable. More information on the gauges is in Table 3.

[21] Monthly flow at these 46 gauges is plotted in Figure 8, with the 5 year moving average shown in blue and the period of interest shaded gray. Casual inspection suggests that many sites experienced increasing streamflow. A trend analysis was performed using the Mann-Kendall test, with the results given in Table 4 (statistically significant trends, at the 5% level, are in bold). Over the month of July, 34 of the 46 sites show an upward trend, but only four are significant; for August, 42 of the 46 sites show an upward trend, with eight being significant; for September, 40 of the 46 sites have an upward trend, with 12 being significant. This result is consistent with our expectations that if the signal of July ΔP can be detected in streamflow records, it could be in July from increased surface runoff but would be more likely in August and September from increased groundwater base flow because the latter accounts for >75% of streamflow in the region.

Figure 6. Maps showing sites of observations used in this study: (a) groundwater wells and soil moisture sites and (b) streamflow gauges (including considered, selected, and dam locations), pan evaporation, and air humidity sites. Bottom color bar gives percent increase in July P.

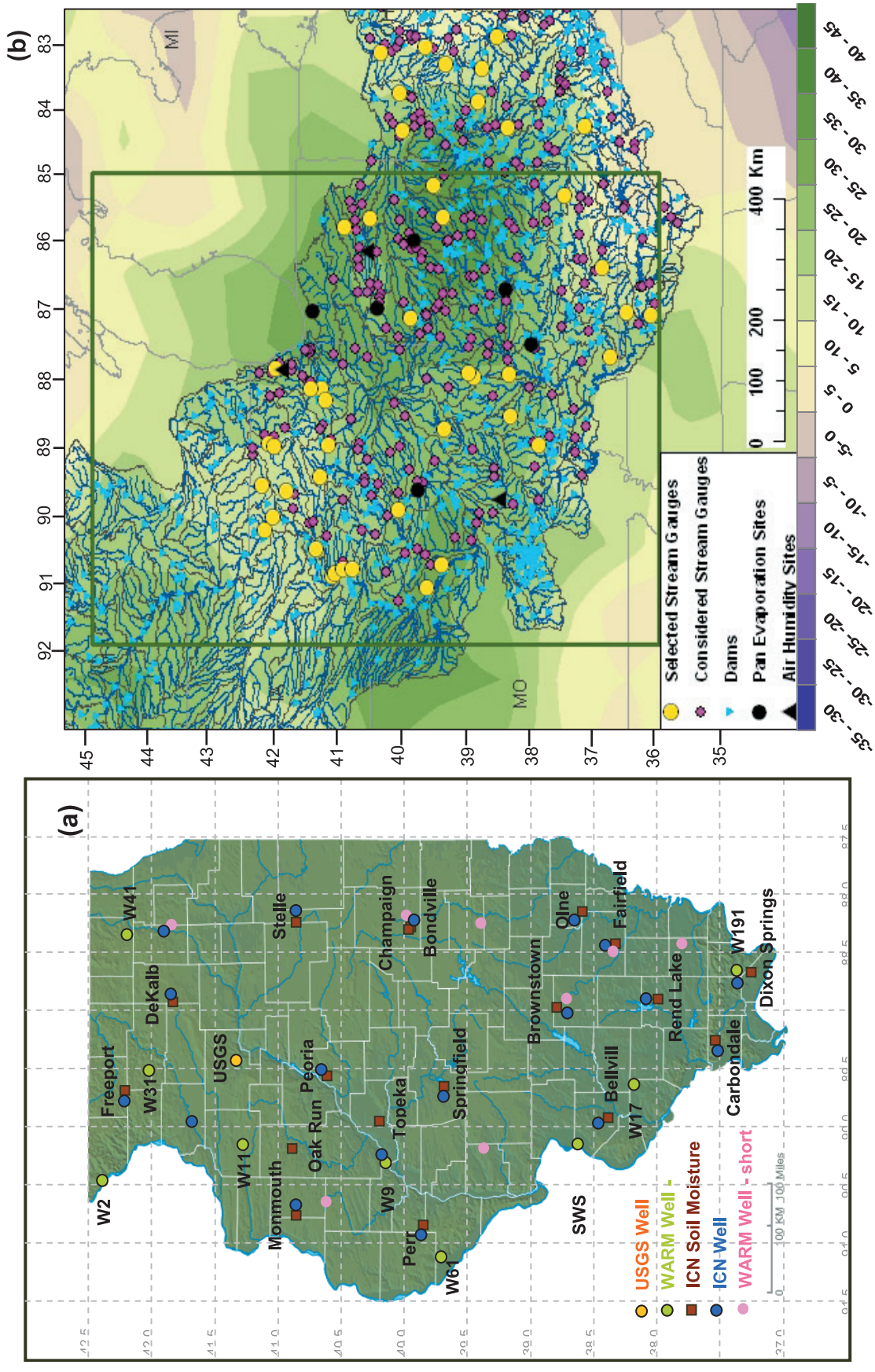
(a)
W2
Freeport
W31
W41
DeKalb
USGS
W11
Monmouth
Stelle
Peoria
Oak Run
W9
Perr
W64
Topeka
Champaign
Bondville
Springfield
Brownstown
Olne
SWS
Fairfield
Bellvill
W17
Rend Lake
Carbondale
W191
Dixon Springs
USGS Well
WARM Well -
ICN Soil Moisture
ICN Well
WARM Well - short
0 100 KM 100 Miles
(b)
MI
MO
Selected Stream Gauges
Considered Stream Gauges
Dams
Pan Evaporation Sites
Air Humidity Sites
0 100 200 400 Km

Figure 6

Table 1. Information on Groundwater Observation Wells Used in This Study[a]

Site	Site Name	Latitude	Longitude	Land Elevation (m)	Well Depth (m)	Begin Year	End Year	Observation Frequency	Mean Water Table Depth (m)
				Wells With Early Data					
USGS 412220089290301	USGS 1	41.37	−89.47	212.75	8.84	1942	1990	10 days	3.34
ISWS-WARM W11	Cambridge			246.98	12.8	1961	2004	monthly	2.91
ISWS-WARM W21	Galena			222.69	7.62	1963	2007	monthly	6.50
ISWS-WARM W31	Mount Morris			282.03	16.76	1960	2007	monthly	5.85
ISWS-WARM W41	Crystal Lake			273.04	5.49	1950	2007	monthly	1.57
ISWS-WARM W61	Barry			190.8	8.53	1956	2007	monthly	3.60
ISWS-WARM W91	Snicarte			148.29	12.8	1958	2007	monthly	11.29
ISWS-WARM W171	Sparta/Eden			156.06	8.23	1960	2007	monthly	2.27
ISWS-WARM W181	SWS 2			128.35	24.38	1952	2004	monthly	4.52
ISWS-WARM W191	Dixon Springs			131.67	2.74	1955	2007	monthly	0.96
Mean									4.28
				Other WARM Wells					
ISWS-WARM W53	Fermi			233.57	4.57	1988	2007	monthly	2.04
ISWS-WARM W72	Good Hope			233.17	9.14	1980	2007	monthly	2.44
ISWS-WARM W132	Greenfield			185.93	6.71	1965	2007	monthly	3.52
ISWS-WARM W143	Janesville			220.52	3.35	1969	2007	monthly	1.66
ISWS-WARM W153	St. Peter			182.27	4.57	1965	2007	monthly	0.94
ISWS-WARM W202	Harrisberg			116.13	3.35	1984	2007	monthly	1.39
ISWS-WARM W221	Boyleston			123.60	7.01	1984	2007	monthly	1.44
ISWS-WARM W1120	Bondville			213.91	6.40	1982	2007	monthly	1.27
Mean									1.84
				ICN Wells at SM Sites					
ISWS-ICN W10	Bellville	38.52	−89.88	133.00	6.10	2000	2010	daily	1.65
ISWS-ICN W1	Bondville	40.05	−88.37	213.00	6.10	2001	2010	daily	1.44
ISWS-ICN W3	Brownstown	38.95	−88.95	177.00	4.57	1997	2010	daily	0.98
ISWS-ICN W11	Carbondale	37.70	−89.23	137.00	7.62	2001	2010	daily	1.53
ISWS-ICN W5	DeKalb	41.85	−88.85	265.00	7.62	1997	2010	daily	1.02
ISWS-ICN W2	Dixon Springs	37.45	−88.67	165.00	2.74	2008	2010	daily	10.28
ISWS-ICN W34	Fairfield	38.38	−88.80	136.00	6.40	2003	2010	daily	0.98
ISWS-ICN W13	Freeport	42.28	−89.67	265.00	7.62	2004	2010	daily	5.28
ISWS-ICN W6	Monmouth	40.92	−90.73	229.00	7.62	1997	2010	daily	4.62
ISWS-ICN W12	Olney	38.73	−88.10	134.00	5.79	2003	2010	daily	1.17
ISWS-ICN W8	Peoria	40.70	−89.52	207.00	12.19	2007	2010	daily	1.56
ISWS-ICN W4	Perry	39.80	−90.83	206.00	6.10	2001	2010	daily	2.48
ISWS-ICN W14	Rend Lake	38.13	−88.92	130.00	6.10	2004	2010	daily	1.46
ISWS-ICN W9	Springfield	39.68	−89.62	177.00	8.53	2004	2010	daily	1.73
ISWS-ICN W15	Stelle	40.95	−88.17	213.00	4.57	2001	2010	daily	0.89
Mean									2.47
				Other ICN Wells					
ISWS-ICN W3	Kilbourne	40.17	−90.08	152.00		2002	2010	daily	9.14
ISWS-ICN W20	St. Charles	41.90	−88.37	226.00		2000	2010	daily	5.99
ISWS-ICN W22	Big Bend	41.64	−90.04	182.00		2005	2009	daily	4.52
Mean									6.55

[a]Wells with early data are shown in Figure 7 and Table 2. USGS, U.S. Geological Survey; ISWS, Illinois State Water Survey; WARM, Water and Atmosphere Resource Monitoring; ICN, Illinois Climate Network.

[22] We assess the field significance of the streamflow trends. The 46 gauges were chosen to be independent of one another by excluding nested basins. The binomial test indicates that similar to water table trends, the streamflow trends are field significant at the 5% level in August and September but not in July. The regional Kendall's S test, if independence cannot be assumed, suggests the same.

[23] Although it may be concluded on the basis of the previous analyses that groundwater storage and streamflow in the study region has increased in August and September since the onset of High Plains irrigation development, we have not yet established a link to the increased July P. Evidence of such a link may be found in the soil moisture, the filter between the climatic forcing and the groundwater-river system.

3.3. Changes in Soil Moisture

[24] SM at 11 levels down to 2 m depth is observed over 1981–2004 at 18 sites across the state of Illinois (Figure 6a, brown symbols). The observations began after the period of irrigation expansion (1940–1980), but a close examination of how, in the postirrigation era, July rainfall propagates through the shallow to the deeper soils in years with above-normal July P may shed some light on whether the July ΔP signal can reach the deeper soil depths and recharge the water table.

[25] Table 5 gives the P anomaly in May–September covering the period of SM observations (1981–2004) based on 316 long-term precipitation station data obtained from the NCDC and averaged over region 3 (Figure 2a). It is calculated as the deviation of monthly P from the

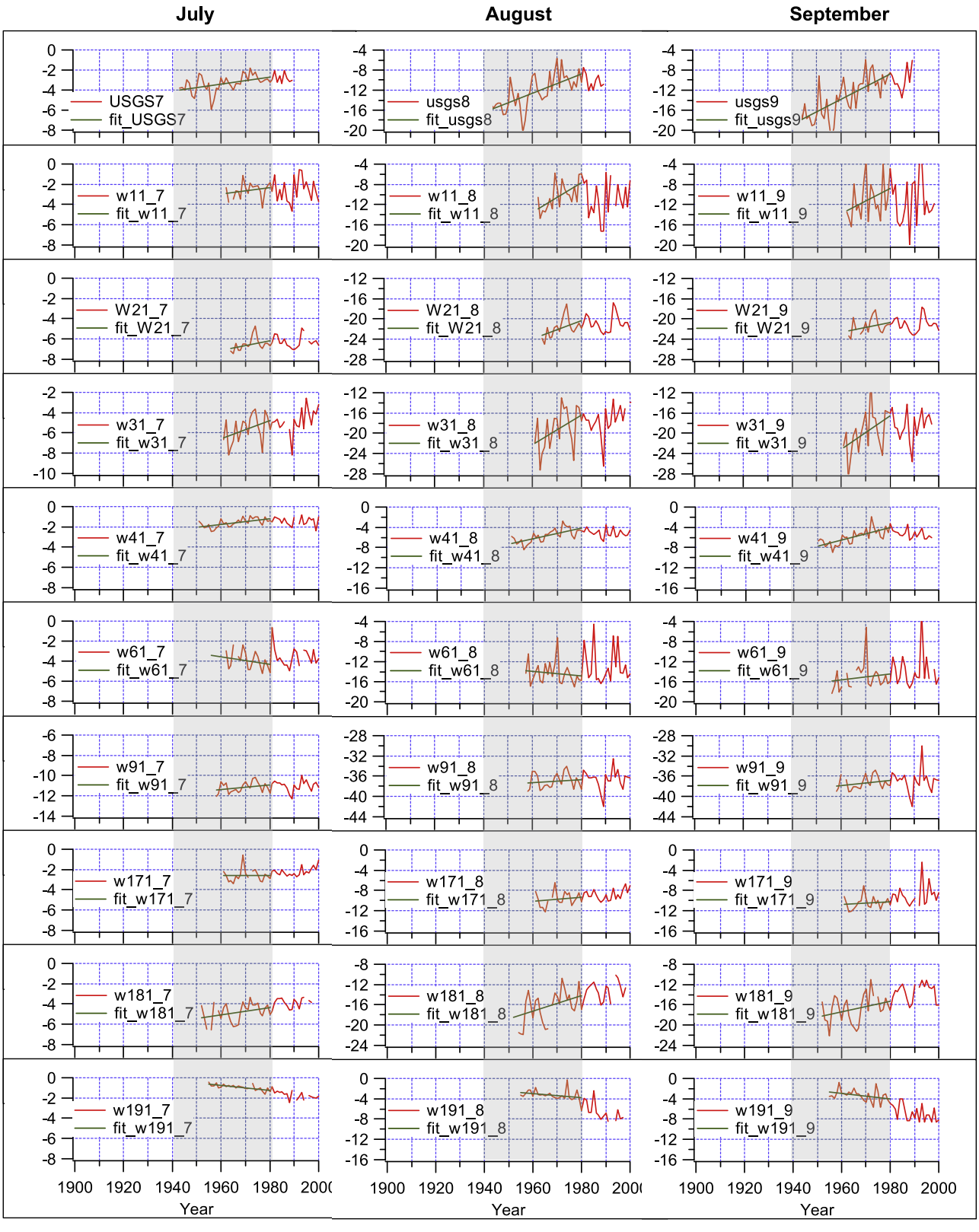

Figure 7. Observed July, August, and September water table depth (m below land surface) at 10 long-term monitoring sites, with a linear regression line fitted to data over 1940–1980.

Table 2. Results of Water Table Trend Analysis Over 1940–1980 Using the Mann-Kendall Test[a]

		July Water Table				August Water Table				September Water Table			
Site	Record Period	Mann-Kendall Test Statistic *S*	*Z* Statistic	*p* Value	Trend	Mann-Kendall Test Statistic *S*	*Z* Statistic	*p* Value	Trend	Mann-Kendall Test Statistic *S*	*Z* Statistic	*p* Value	Trend
USGS1	1943–1990	−237	−2.9670	0.00	**rising**	−343	−4.2996	0.00	**rising**	−353	−4.4253	0.00	**rising**
W11	1962–2004	−45	−1.6666	0.10	rising	−75	−2.5889	0.01	**rising**	−39	−1.3295	0.18	rising
W21	1963–2006	−44	−1.7713	0.08	rising	−51	−2.0614	0.04	**rising**	−34	−1.3594	0.17	rising
W31	1961–2006	−52	−1.6547	0.10	rising	−54	−1.7195	0.09	rising	−62	−1.9791	0.05	**rising**
W41	1950–2006	−203	−3.6039	0.00	**rising**	−219	−3.8893	0.00	**rising**	−246	−4.1647	0.00	**rising**
W61	1956–2006	54	1.6004	0.11	falling	39	1.0036	0.32	falling	−37	−0.9508	0.34	rising
W91	1958–2006	−45	−1.1621	0.25	rising	−35	−0.8980	0.37	rising	−53	−1.4663	0.14	rising
W171	1961–2006	−5	−0.1399	0.89	rising	−17	−0.5598	0.58	rising	−33	−1.0388	0.30	rising
W181	1955–2006	−63	−1.2925	0.20	rising	−81	−1.7633	0.08	rising	−55	−1.1257	0.26	rising
W191	1952–2006	163	3.7845	0.00	**falling**	126	2.7559	0.01	**falling**	70	1.5212	0.13	falling

[a]Bold indicates statistically significant at the 5% level.

Table 3. Information on the 46 Stream Gauges Used in This Study

Gauge Site	USGS Gauge	Latitude	Longitude	State	Record Period	River Name	Drainage Area (km^2)
1	3345500	38.9364	−88.0225	Illinois	1915–2009	Embarras River	3,926
2	3380500	38.3583	−88.5847	Illinois	1909–2008	Skillet Fork	1,202
3	3346000	39.0100	−87.9456	Illinois	1941–2009	North Fork Embarras River	824
4	3378000	38.3864	−87.9756	Illinois	1941–2009	Bonpas Creek	591
5	5419000	42.25278	−90.28583	Illinois	1935–1977	Apple River	640
6	5420000	42.11417	−90.09278	Illinois	1941–1977	Plum River	596
7	5435500	42.30278	−89.61944	Illinois	1915–2009	Pecatonica River	3,434
8	5440000	42.19444	−88.99889	Illinois	1940–2009	Kishwaukee River	2,846
9	5440500	42.09889	−89.05194	Illinois	1940–1971	Killbuck Creek	303
10	5444000	41.90278	−89.69611	Illinois	1940–2009	Elkhorn Creek	378
11	5448000	41.44222	−90.55583	Illinois	1940–2008	Mill Creek	162
12	5466500	41.18694	−90.96722	Illinois	1935–1972	Edwards River	1,153
13	5467000	41.12889	−90.91917	Illinois	1935–2009	Pope Creek	451
14	5469000	41.00139	−90.85417	Illinois	1935–2009	Henderson Creek	1,119
15	5469500	40.85694	−90.86389	Illinois	1940–1971	South Henderson Creek	215
16	5502040	39.69306	−91.14861	Illinois	1940–1986	Hadley Creek	188
17	5513000	39.44306	−90.79583	Illinois	1940–1986	Bay Creek	383
18	5527500	41.34667	−88.18639	Illinois	1915–2009	Kankakee River	13,338
19	5529000	42.08167	−87.89056	Illinois	1941–2009	Des Plaines River	932
20	5540500	41.52222	−88.19250	Illinois	1941–2008	Du page River	839
21	5542000	41.28611	−88.35972	Illinois	1940–2009	Mazon River	1,178
22	5555500	41.25528	−89.01222	Illinois	1932–1971	Vermilion River	3,310
23	5556500	41.36583	−89.49833	Illinois	1936–2009	Big Bureau Creek	508
24	5583000	40.12417	−89.98500	Illinois	1940–2009	Sangamon River	15,289
25	5592000	39.40722	−88.78139	Illinois	1941–1970	Kaskaskia River	2,730
26	5597000	37.90139	−89.01389	Illinois	1908–1971	Big Muddy River	2,056
27	3326500	40.5764	−85.6600	Indiana	1924–2009	Mississinewa River	1,766
28	3340000	39.9311	−87.1258	Indiana	1941–1971	Sugar Creek	1,735
29	3275000	39.5794	−85.1581	Indiana	1929–2009	Whitewater River	1,352
30	3328000	40.9939	−85.7814	Indiana	1930–2009	Eel River	1,080
31	3363500	39.4175	−85.6342	Indiana	1931–2009	Flatrock River	785
32	3252500	38.3908	−84.3031	Kentucky	1938–2009	South Fork Licking River	1,608
33	3406500	37.1711	−84.2961	Kentucky	1936–2009	Rockcastle River	1,564
34	3314000	36.8953	−86.3806	Kentucky	1941–1971	Drakes Creek	1,238
35	3438000	36.7778	−87.7217	Kentucky	1940–2009	Little River	632
36	3217000	38.5642	−82.9522	Kentucky	1941–2009	Tygarts Creek	627
37	3299000	37.4972	−85.3239	Kentucky	1938–1992	Rolling Fork	619
38	3219500	40.4194	−83.1972	Ohio	1925–2010	Scioto River	1,469
39	3230500	39.7006	−83.1103	Ohio	1922–2009	Big Darby Creek	1,383
40	3265000	40.0578	−84.3561	Ohio	1917–2009	Stillwater River	1,303
41	3237500	38.8036	−83.4211	Ohio	1926–2010	Ohio Brush Creek	1,002
42	3232000	39.3792	−83.3756	Ohio	1927–2009	Paint Creek	645
43	3238500	38.8581	−83.9286	Ohio	1925–2009	White Oak Creek	565
44	3267000	40.1075	−83.7992	Ohio	1926–2009	Mad River	420
45	3434500	36.1219	−87.0989	Tennessee	1926–2009	Harpeth River	1,764
46	3436000	36.5153	−87.0589	Tennessee	1939–1991	Sulphur Fork Red River	482

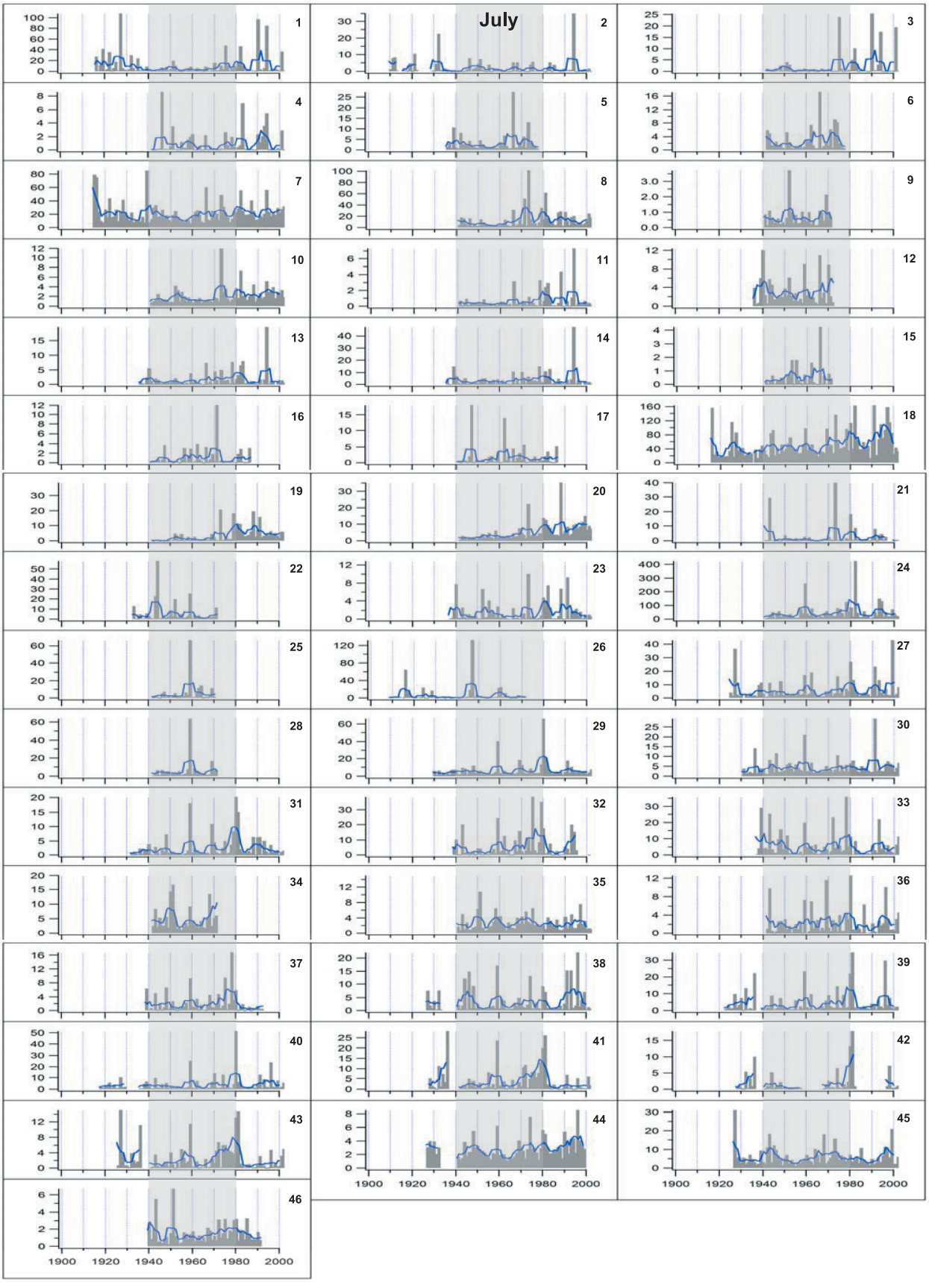

Figure 8. Observed July–September streamflow at 46 gauges. Blue curves are 5 year moving averages to show the long-term variability.

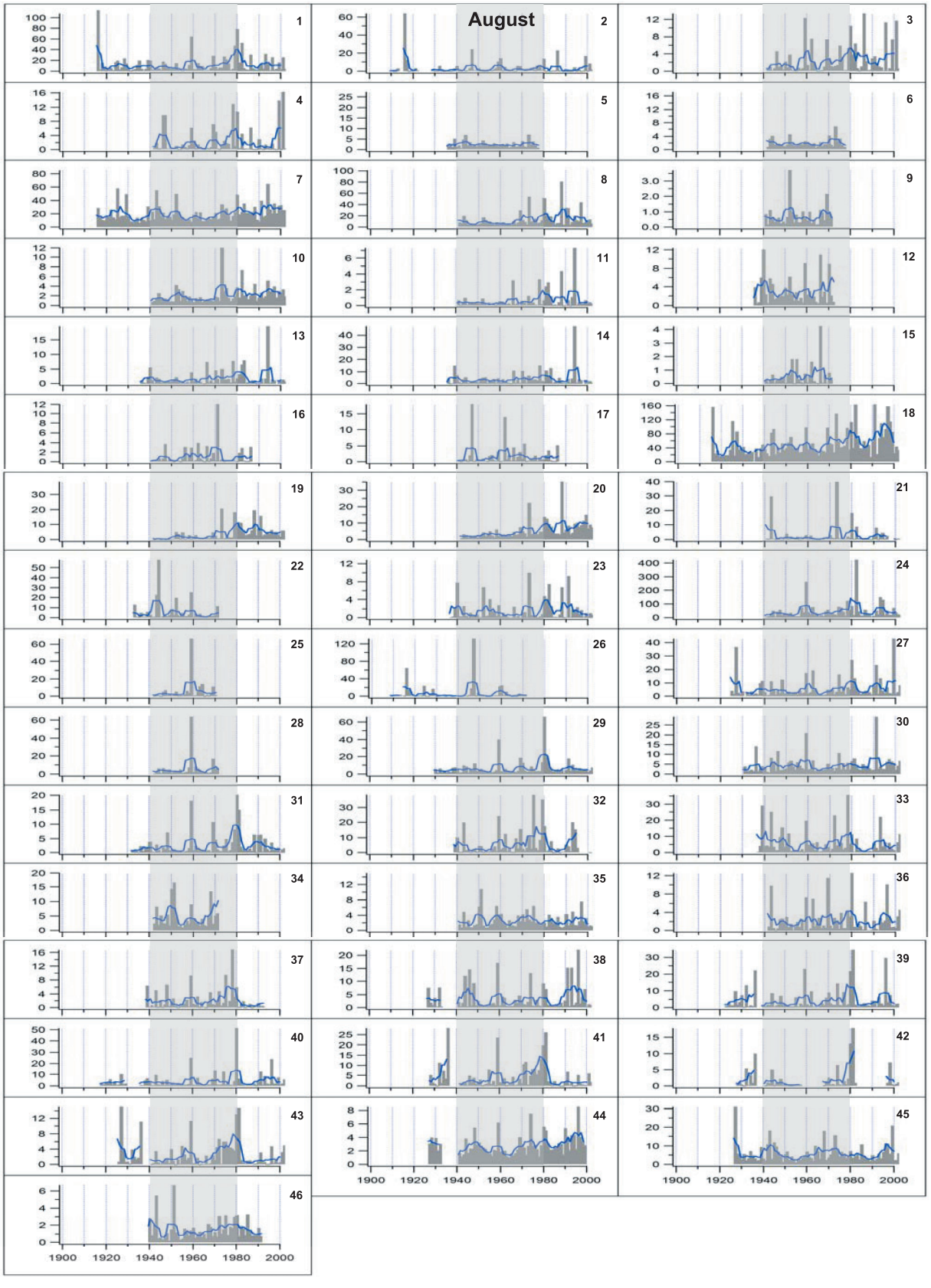

Figure 8. (continued)

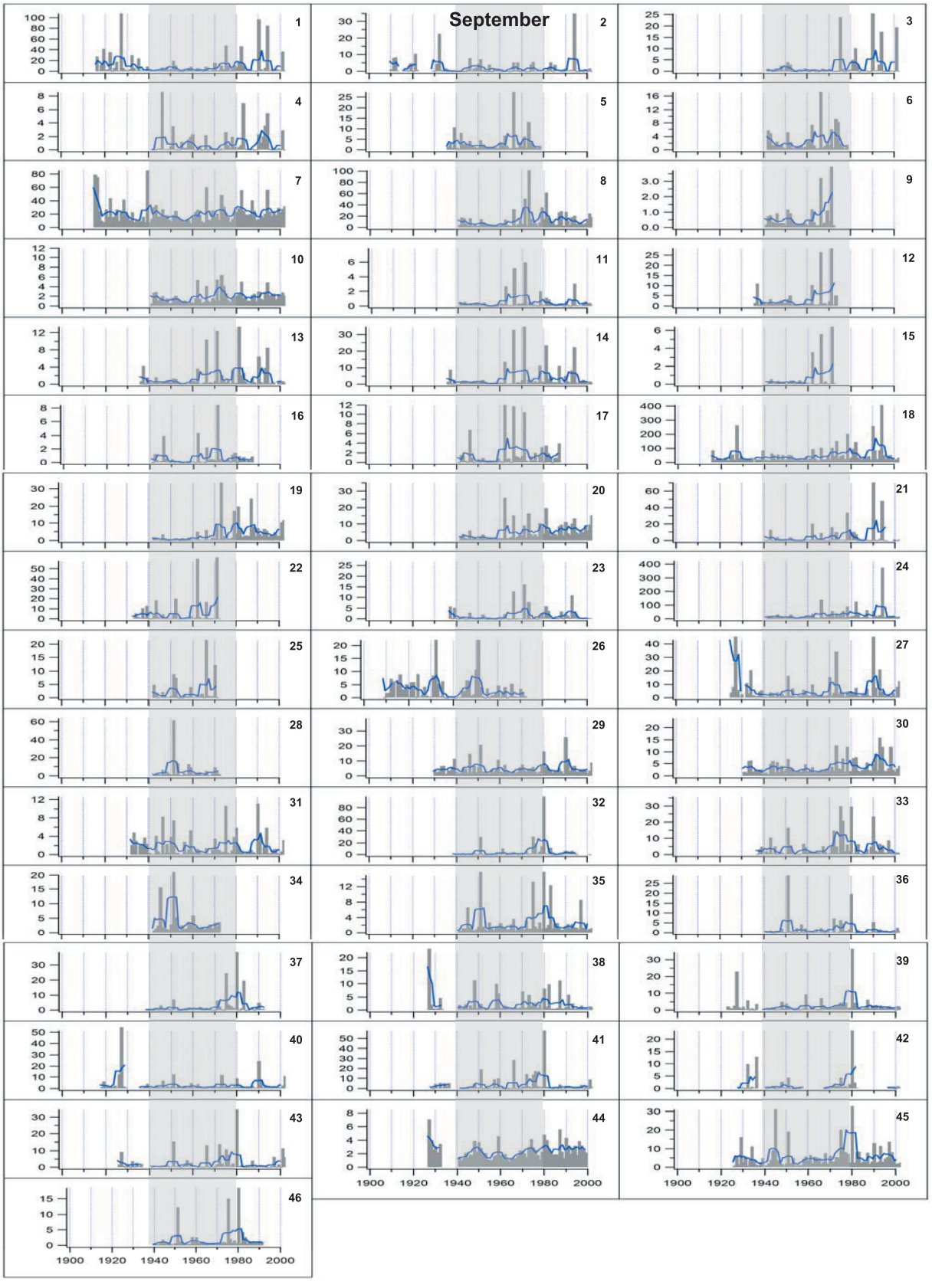

Figure 8. (continued)

Table 4. Results of Streamflow Trend Analysis Over 1940–1980 Using the Mann-Kendall Test[a]

				July Streamflow				August Streamflow				September Streamflow			
Stream Sites	State	Record Period	Basin Area (km^2)	Mann-Kendall Test Statistic S	Z Statistic	p Value	Trend	Mann-Kendall Test Statistic S	Z Statistic	p Value	Trend	Mann-Kendall Test Statistic S	Z Statistic	p Value	Trend
1	Illinois	1915–2009	3926	12	0.1236	0.900	increasing	178	1.9881	0.047	**increasing**	166	1.8533	0.064	Increasing
2	Illinois	1909–2008	1202	42	0.4605	0.650	increasing	102	1.1344	0.257	increasing	−4	−0.0337	0.739	Decreasing
3	Illinois	1941–2009	824	98	1.1302	0.258	increasing	156	1.8059	0.071	increasing	18	0.1981	0.842	Increasing
4	Illinois	1941–2009	591	100	1.1535	0.248	increasing	98	1.1302	0.258	increasing	75	0.8622	0.389	Increasing
5	Illinois	1935–1977	640	3	0.0251	0.979	increasing	−47	−0.5783	0.563	decreasing	−27	−0.3269	0.744	Decreasing
6	Illinois	1941–1977	596	10	0.1177	0.906	increasing	18	0.2223	0.824	increasing	10	0.1177	0.906	Increasing
7	Illinois	1915–2009	3434	8	0.0786	0.937	increasing	−12	−0.1236	0.902	decreasing	34	0.3707	0.711	Increasing
8	Illinois	1940–2009	2846	190	2.1228	0.033	**increasing**	182	2.0330	0.042	**increasing**	150	1.6736	0.094	Increasing
9	Illinois	1940–1971	303	90	1.4433	0.149	increasing	18	0.2757	0.783	increasing	−10	−0.1459	0.884	Decreasing
10	Illinois	1940–2009	378	200	2.2352	0.025	**increasing**	146	1.6286	0.103	increasing	144	1.6062	0.108	Increasing
11	Illinois	1940–2008	162	−4	−0.0337	0.973	decreasing	35	0.3819	0.703	increasing	62	0.6851	0.493	Increasing
12	Illinois	1935–1972	1153	−36	−0.5423	0.587	decreasing	4	0.0465	0.963	increasing	0	0.0000	1.000	Increasing
13	Illinois	1935–2009	451	−48	−0.5279	0.597	decreasing	108	1.2018	0.229	increasing	84	0.9323	0.351	Increasing
14	Illinois	1935–2009	1119	−8	−0.0786	0.937	decreasing	124	1.3815	0.167	increasing	132	1.4714	0.141	Increasing
15	Illinois	1940–1971	215	−94	−1.5081	0.131	decreasing	2	0.0162	0.987	increasing	−6	−0.0811	0.935	Decreasing
16	Illinois	1940–1986	188	−28	−0.3033	0.762	decreasing	−9	−0.0899	0.928	decreasing	106	1.1794	0.238	Increasing
17	Illinois	1940–1986	383	−32	−0.3482	0.727	decreasing	140	1.5612	0.119	increasing	164	1.8308	0.067	Increasing
18	Illinois	1915–2009	13,338	50	0.5504	0.582	increasing	130	1.4489	0.147	increasing	185	2.0668	0.039	**Increasing**
19	Illinois	1941–2009	932	202	2.3419	0.019	**increasing**	324	3.7633	0.000	**increasing**	314	3.6468	0.000	**Increasing**
20	Illinois	1941–2008	839	276	3.2040	0.001	**increasing**	342	3.9730	0.000	**increasing**	319	3.7053	0.000	**Increasing**
21	Illinois	1940–2009	1178	74	0.8199	0.412	increasing	108	1.2018	0.229	increasing	308	3.4482	0.001	**Increasing**
22	Illinois	1932–1971	3310	24	0.3730	0.709	increasing	−50	−0.7946	0.427	decreasing	−14	−0.2108	0.833	Decreasing
23	Illinois	1936–2009	508	−38	−0.4156	0.677	decreasing	10	0.1011	0.920	increasing	128	1.4265	0.154	Increasing
24	Illinois	1940–2009	15,289	−8	−0.0786	0.937	decreasing	168	1.8757	0.061	increasing	186	2.0779	0.038	**Increasing**
25	Illinois	1941–1970	2730	−55	−0.9634	0.335	decreasing	31	0.5352	0.593	increasing	7	0.1070	0.915	Increasing
26	Illinois	1908–1971	2056	18	0.2757	0.782	increasing	2	0.0162	0.987	increasing	−26	−0.4054	0.685	Decreasing
27	Indiana	1924–2009	1766	52	0.5728	0.566	increasing	158	1.7634	0.078	increasing	196	2.1902	0.029	**Increasing**
28	Indiana	1941–1971	1735	59	0.9858	0.324	increasing	43	0.7138	0.475	increasing	37	0.6119	0.541	Increasing
29	Indiana	1929–2009	1352	120	1.3366	0.181	increasing	132	1.4714	0.141	increasing	132	1.4714	0.141	Increasing
30	Indiana	1930–2009	1080	8	0.0786	0.937	increasing	89	0.9885	0.323	increasing	144	1.6062	0.108	Increasing
31	Indiana	1931–2009	785	132	1.4714	0.141	increasing	194	2.1678	0.030	**increasing**	116	1.2917	0.196	Increasing
32	Kentucky	1938–2009	1608	108	1.2018	0.229	increasing	240	2.6844	0.007	**increasing**	280	3.1337	0.002	**Increasing**
33	Kentucky	1936–2009	1564	−42	−0.4605	0.645	decreasing	8	0.0786	0.937	increasing	168	1.8757	0.061	Increasing
34	Kentucky	1941–1971	1238	29	0.4759	0.634	increasing	40	0.6630	0.507	increasing	39	0.6459	0.518	Increasing
35	Kentucky	1940–2009	632	46	0.5054	0.613	increasing	85	0.9435	0.345	increasing	119	1.3255	0.185	Increasing
36	Kentucky	1941–2009	627	36	0.4078	0.683	increasing	78	0.8971	0.370	increasing	176	1.9656	0.049	**Increasing**
37	Kentucky	1938–1992	619	−51	−0.5616	0.574	decreasing	144	1.6062	0.108	increasing	178	1.9881	0.046	**Increasing**
38	Ohio	1925–2010	1469	42	0.4605	0.645	increasing	55	0.6066	0.544	increasing	148	1.6511	0.099	Increasing
39	Ohio	1922–2009	1383	90	0.9996	0.317	increasing	173	1.9320	0.053	increasing	240	2.6844	0.007	**Increasing**
40	Ohio	1917–2009	1303	66	0.7301	0.465	increasing	58	0.6402	0.522	increasing	122	1.3591	0.174	Increasing
41	Ohio	1926–2010	1002	110	1.2700	0.204	increasing	276	3.2040	0.001	**increasing**	168	1.9457	0.052	Increasing
42	Ohio	1927–2009	645	99	1.6656	0.095	increasing	85	1.4277	0.153	increasing	165	2.7874	0.005	**Increasing**
43	Ohio	1925–2009	565	148	1.6511	0.099	increasing	268	2.9989	0.003	**increasing**	138	1.5388	0.124	Increasing
44	Ohio	1926–2009	420	142	1.5837	0.113	increasing	94	1.0446	0.296	increasing	148	1.6511	0.099	Increasing
45	Tennessee	1926–2009	1764	100	1.1120	0.266	increasing	36	0.3931	0.694	increasing	202	2.2576	0.024	**Increasing**
46	Tennessee	1939–1991	482	132	1.4714	0.141	increasing	170	1.8982	0.058	increasing	109	1.2131	0.225	Increasing

[a]Bold indicates statistically significant at the 5% level.

Table 5. Warm Season Precipitation Anomaly (%) Based on the Mean of 316 Station Records in Region 3 Over the Period of 1980–2004 When Soil Moisture Observations Are Available[a]

Year	May	June	July	August	September
1980	−0.346	0.035	−0.154	0.451	0.276
1981	0.141	0.206	0.319	0.290	−0.094
1982	−0.064	−0.094	0.226	0.137	−0.174
1983	0.329	−0.264	−0.392	−0.300	−0.159
1984	0.091	−0.273	−0.125	−0.407	0.237
1985	−0.242	−0.039	−0.193	0.338	−0.132
1986	0.005	0.000	0.243	−0.228	0.977
1987	−0.365	−0.198	0.161	0.266	−0.263
1988	−0.630	−0.748	−0.157	−0.141	0.063
1989	−0.088	−0.084	−0.044	0.047	0.094
1990	0.442	0.335	−0.045	0.165	−0.277
1991	−0.016	−0.451	−0.247	−0.224	−0.072
1992	−0.565	−0.444	0.607	−0.283	0.481
1993	−0.147	0.565	0.325	0.295	0.776
1994	−0.513	0.047	−0.061	0.011	−0.186
1995	0.515	−0.155	−0.176	0.190	−0.497
1996	0.335	0.223	0.049	−0.450	0.182
1997	0.010	0.104	−0.288	0.147	−0.249
1998	−0.111	0.764	0.010	−0.013	−0.393
1999	−0.197	0.087	−0.014	−0.338	−0.463
2000	0.109	0.548	−0.013	−0.025	0.147
2001	0.083	−0.005	−0.063	0.090	0.159
2002	0.363	−0.022	−0.257	0.032	−0.053
2003	0.223	−0.113	0.214	−0.238	0.323
2004	0.638	−0.024	0.076	0.189	−0.702

[a]The anomaly is calculated as monthly P deviation from the 1980–2004 mean divided by the mean. The years 1986, 1992, and 2003 are examined. Region 3 is shown as a green box in Figure 2a.

1980–2004 mean and divided by the mean (i.e., (P − mean)/mean). We examine three years, 1986, 1992, and 2003, when a wet July is sandwiched between a normal or dry June and a dry August. Here any positive anomaly in the soil moisture may be attributable to the above-normal July P, allowing us to see whether a positive July P anomaly alone can reach the deep soil.

[26] Biweekly soil moisture observations in Illinois are obtained from the Global Soil Moisture Databank (http://climate.envsci.rutgers.edu/soil_moisture/illinois.html) at three depths: 0.1–0.3, 0.9–1.1, and 1.7–1.9 m. The topmost (0–0.1 m) and bottommost (1.9–2.0 m) layers have many missing data; hence, the next shallowest and deepest layers are used. Soil moisture anomaly is calculated for each site and month as the deviation from the mean divided by the mean, the latter being obtained from the entire record (1981–2004) for each site for the respective layer and month. The regional anomaly is then calculated as the mean anomaly of the 18 sites. Figure 9 plots the P and SM anomalies at three depths over the warm season of the three years.

[27] In 1986 (Figure 9a), the entire soil moisture profile is near normal in June because of the near-normal P in both May and June. The above-normal July P not only wetted the shallow soil but also elevated the deeper soils to above normal. This positive anomaly in the deeper soils persisted into August despite the below-normal August P. The July P anomaly here (24.3% increase) is at a similar magnitude to the July ΔP signal (Figure 2a). In 1992 (Figure 9b), despite the large precipitation and soil water deficit in May and June, the above-normal July P wetted the deepest soil layer to above normal, which persisted into August despite the large deficit in August P. In 2003, the below-normal soil moisture in the deep layers in June is elevated to above-normal values by the above-normal July P. These cases suggest that a positive July P can reach the deeper soils (1.7–1.9 m) despite the normal to dry antecedent soil moisture conditions and high ET rates in July and August.

[28] Water table observations are available at 15 Illinois Climate Network (ICN) wells collocated with 14 of the 18 soil moisture sites used in the above analyses (Figure 6a and the ICN wells at SM sites in Table 1). The temporal (over 1998–2009) and spatial (over 15 sites) mean water table depth at these ICN wells is 2.47 m, not far from the 1.7–1.9 m soil layer analyzed above. To further characterize the groundwater conditions in Illinois, we compiled observations from a total of 34 wells, including the 10 historic wells used in the trend analyses earlier (wells with early data in Table 1), the shorter ISWS-WARM well records (other WARM wells), the 15 ICN wells collocated with soil moisture sites (ICN wells at SM sites), and the rest of the ICN wells (other ICN wells). All data are maintained by ISWS (see http://www.isws.illinois.edu/warm/sgwdata/wells.aspx) except for the USGS well, and their locations are shown in Figure 6a. The temporal mean at the 34 wells gives the frequency distribution of water table depth in space shown in Figure 9d. It suggests that the water table in Illinois clusters around the 1–2 m depth, with 53% of the sites <2 m and 68% <3 m deep. If the above-normal July P in 1986, 1992, and 2003 could reach the soils at the 1.7–1.9 m depth with normal to dry antecedent soil moisture conditions, then the July ΔP signal might have also reached the shallow water table, at least in the years with normal to wet antecedent soil moisture conditions.

3.4. Changes in ET

[29] Last, we address the role of possible changes in ET. The increased groundwater storage and streamflow in August–September could have been caused by the increased July P, but it also could have been caused by reduced July ET because it is P − ET, the net soil water surplus, that reaches the water table. Since actual ET is not routinely and historically observed, we infer changes in ET from changes in those variables that are historically observed and indicative of ET, such as maximum air temperature, pan evaporation, air relative humidity, and atmospheric vapor density deficit computed from the latter two.

[30] July mean daily maximum air temperature (T_{max}) averaged over 104 station records in the states of Illinois and Indiana (data from the NCDC) is plotted in Figure 10a. A notable cooling began in the mid-1950s and continued to the late 1970s. This is consistent with the observed U.S. [e.g., *Liepert*, 2002] and global-scale cooling due to reduced solar radiation over the period of 1950–1980 (i.e., solar dimming; see recent review by *Wild* [2009]) caused by changes in anthropogenic aerosols and their interaction with changes in clouds. In the central United States, the cooling has also been linked to large-scale land use changes such as converting forest to crops and, particularly, irrigation [e.g., *Bonan*, 2001; *Govindasamy et al.*, 2001; *Milly and Dunne*, 2001; *Baidya Roy et al.*, 2003; *Boucher et al.*, 2004; *Feddema et al.*, 2005; *Lobell et al.*, 2006, 2008; *Adegoke et al.*, 2007; *Kueppers et al.*, 2007; *Diffenbaugh*,

2009]. The mechanisms include the higher albedo (reflecting more solar radiation) of croplands, increased latent versus sensible heat due to irrigation, and, indirectly, increased cloud cover caused by higher ET. A recent global model simulation study [*Puma and Cook*, 2010] forced by observed sea surface temperature and reconstructed global irrigation development history shed much light on the cause of the cooling by illustrating that cooling occurred in both the irrigation and nonirrigation ensemble simulations but more so in the ensemble with irrigation. Although the causes might have been multiple, the cooling is certain.

[31] The relevance of this cooling to the present study is that ET might have been reduced since the 1950s, allowing deeper infiltration and water table recharge, without additional precipitation. Records of observed pan evaporation, a direct indicator of atmospheric ET demand, are available from six stations in Illinois and Indiana (from the NCDC) dating back to at least the 1950s and continuing to the 1980s. Figure 10b plots the July total pan evaporation at these six sites, and Table 6 gives the site information and the result of the Mann-Kendall trend analysis. There are no statistically significant (at the 5% level) trends in any of these records, suggesting that the cooling alone may not have caused a change in the atmospheric ET demand.

[32] To supplement these few pan evaporation records, we assessed changes in ET demand by computing the atmospheric vapor pressure deficit (VPD) from relative humidity (RH) and air temperature (T_a) records. We found long-term observations of air humidity at only three stations from the NCDC archive; most of the long-term records have a data gap (1948–1973) over our period of interest (1940–1980), unfortunately. The VPD is computed as

$$\mathrm{VPD} = e^*(1 - \mathrm{RH}/100),$$
$$e^* = 0.611 \exp\left(\frac{17.3 T_a}{237.3 + T_a}\right), \quad (1)$$

where e^* (kPa) is the saturation vapor pressure at air temperature T_a (°C). Figure 10c plots the July T_a, RH, and VPD (with 5 year moving averages). At first glance, the two short records suggest an upward VPD trend over 1940–1980, though the lack of data in the 1940s and 1950s makes them difficult to judge. On the basis of a trend analysis (Table 7), no significant trends (at the 5% level) are found at the three sites.

[33] However, neither pan evaporation nor VPD are sufficient to infer the actual ET because they only tell half of the story (the atmospheric demand side); soil water availability (or the land supply side) can be the dominate control where ET is water limited. The relationships among pan evaporation, VPD, and actual ET are complex and multidimensional, involving land-atmosphere feedbacks, vegetation and land cover, and changes in the dominant forcing [e.g., *Brutsaert and Parlange*, 1998; *Lawrimore and Peterson*, 2000; *Teuling et al.*, 2009; *van Heerwaarden et al.*, 2010]. Nevertheless, actual ET in the region has likely

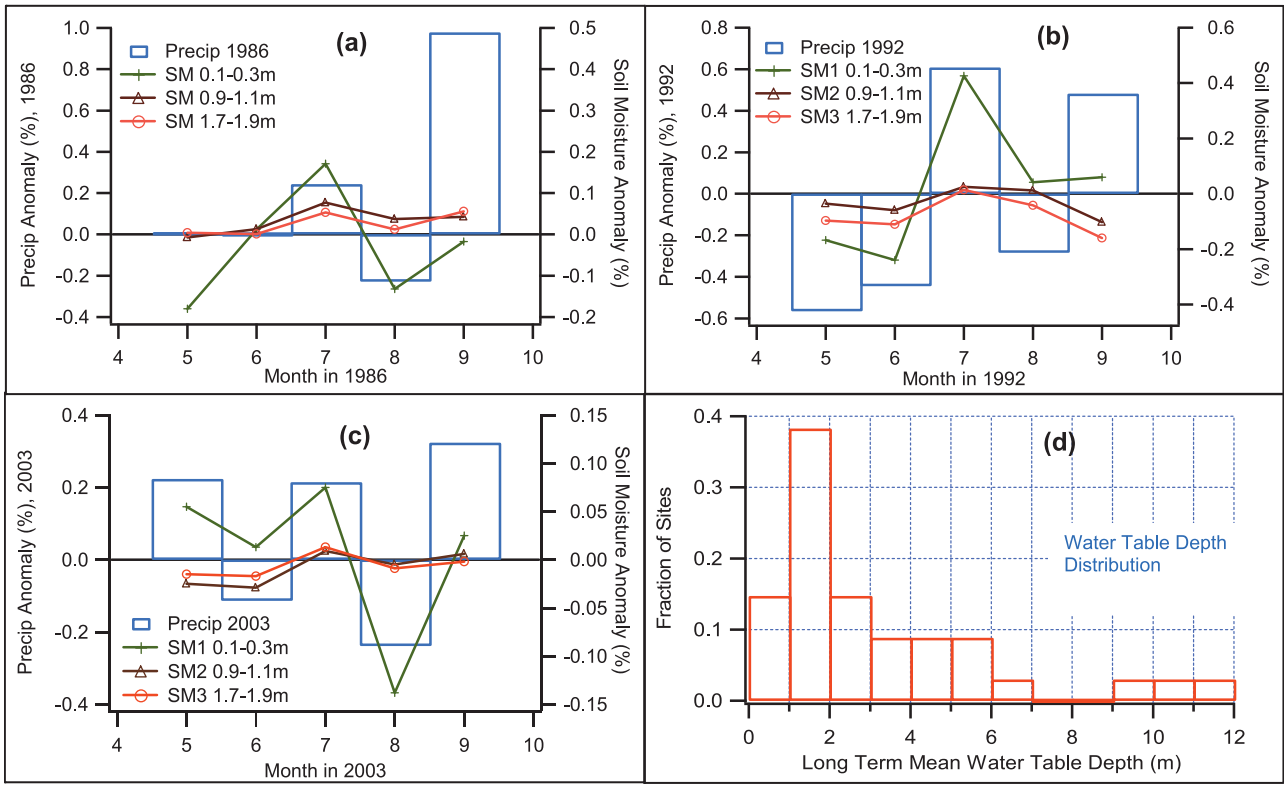

Figure 9. Anomalies in regional mean precipitation (based on 316 station records) and soil moisture (based on 18 site observations) at three depths, May–September of (a) 1986, (b) 1992, and (c) 2003. (d) The long-term mean water table depth distribution based on 34 wells in Illinois (data source is USGS and Water and Atmosphere Resource Monitoring and Illinois Climate Network groundwater monitoring networks, both run by Illinois State Water Survey (data in Table 1)).

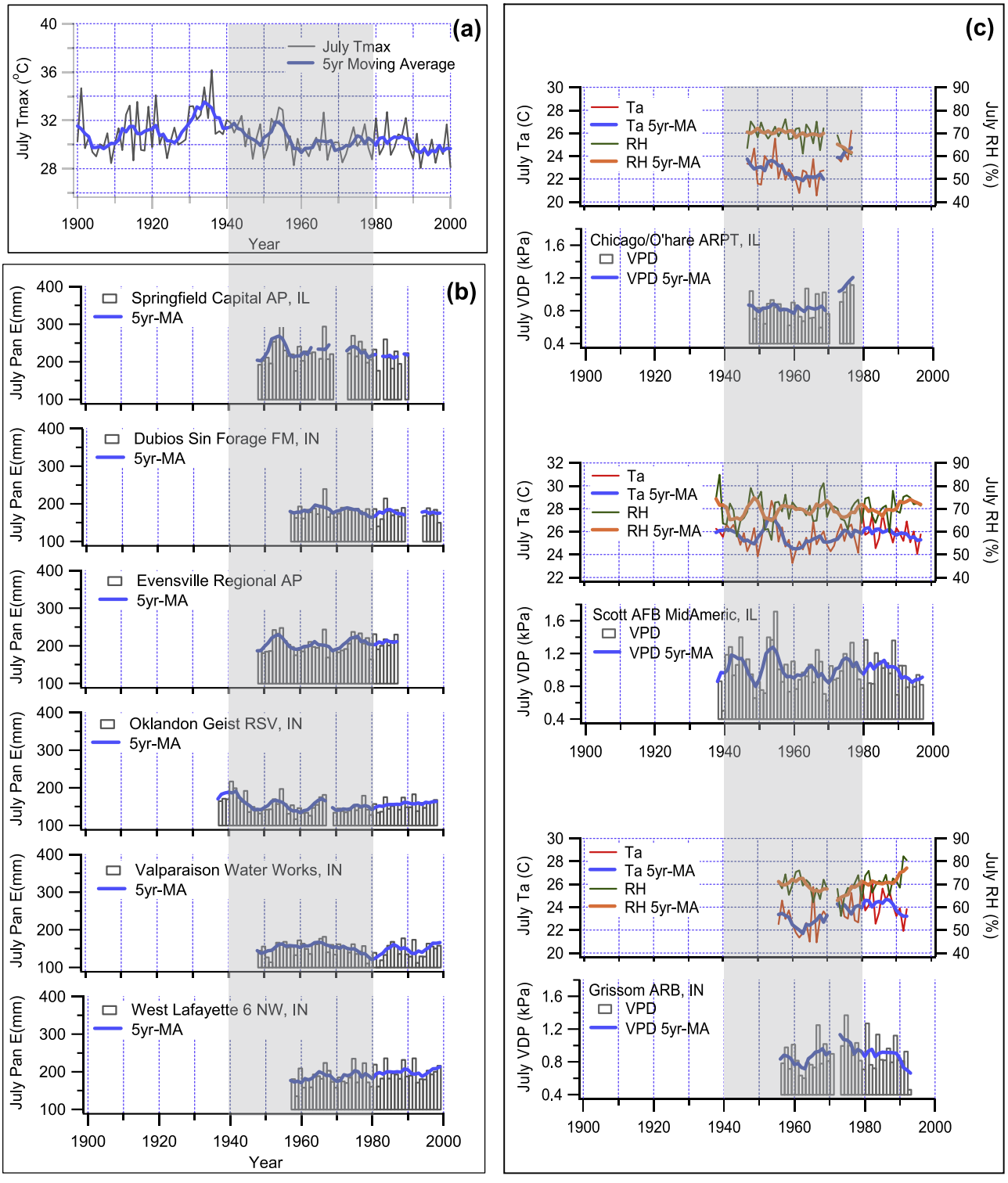

Figure 10. (a) July mean maximum daily temperature (°C) averaged over 104 stations, (b) station pan evaporation (mm) at five sites, and (c) surface air temperature, humidity, and vapor pressure deficit at three sites (5 year moving average is in blue; period of interest is shaded gray).

increased, rather than decreased, over the period of 1940–1980 for the following reasons.

[34] First, the available pan evaporation and VPD records in the region suggest no significant changes in atmospheric ET demand in July (Figures 10 and 11 and Tables 6 and 7). If the atmospheric demand stayed the same, then any changes in the actual ET would have been caused by changes in soil water availability. This is to assume that wind speed and land cover have not changed significantly or they are a weak driver of ET. It has been shown that ET is insensitive to reduction of wind speed (or stilling [see *van Heerwaarden et al.*, 2010]). Since

Table 6. July Pan Evaporation Site Information and Mann-Kendall Test Results for Trends Over 1940–1980[a]

								July Pan Evaporation			
Coop ID	Site Name	State	Latitude	Longitude	Elevation (m)	Period	Mean (mmol)	Mann-Kendall Test Statistic S	Z Statistic	p Value	Trend
118179	Springfield Capital AP	Illinois	39.83	−89.68	181	1948–1990	227	36	0.6920	0.49	increasing
122309	Dubois S in Forage FM	Indiana	38.45	−86.70	210	1957–1999	180	13	0.2980	0.77	increasing
122738	Evansville Regional AP	Indiana	38.03	−87.52	122	1948–1987	205	58	0.8836	0.38	increasing
126506	Oaklandon Geist RSVR	Indiana	39.90	−85.98	242	1937–1998	159	−119	−1.3755	0.17	decreasing
128999	Valparaiso WTR WKS	Indiana	41.50	−87.03	244	1948–1999	150	−62	−0.9457	0.34	decreasing
129430	West Lafayette 6 NW	Indiana	40.47	−86.98	218	1957–1999	192	33	0.7947	0.43	increasing

[a]No significant trends (at the 5% level) are found at the six sites. Coop ID, cooperative station ID.

precipitation has increased, soil should be wetter, in general. Hence, if actual ET has changed at all, it is more likely that it has increased rather than decreased.

[35] Second, the idea that the actual ET in the region is driven by precipitation rather than temperature is supported by a simple and elegant study by *Teuling et al.* [2009], who conclude that changes in actual ET are governed by changes in its key driver (or limiting factor) in a given region. That study shows that annual ET in the central United States, inferred from flux tower and multimodel syntheses, is far more responsive to changes in P than changes in radiation. If this holds true for annual ET, it must hold true for warm season ET because the latter is more water limited than all season ET (Figure 3a, $P <$ ET in warm season).

[36] Third, the annual river basin water balance analyses in the same study [*Teuling et al.*, 2009] demonstrate that ET has increased over the period of solar dimming in the upper Mississippi (including Illinois) and the Ohio river basins. The upward trend in annual ET is explained by the upward trend in annual P, which is partitioned into both increased ET and increased streamflow, as has been shown by *Milly and Dunne* [2001] and *Qian et al.* [2007] over the same region and period. Summer ET dominates annual ET, and if annual ET has increased, then summer ET has likely increased as well.

[37] Thus, it is plausible that the increased July P caused both increased ET and increased streamflow. This is corroborated by our earlier seasonal analysis, which suggested that ET was likely to increase in response to the July ΔP signal because ET exceeds P and there is a net soil water deficit in the warm season. It is also consistent with our earlier soil moisture analysis, which shows that present day above-normal July P could reach the deep soil in dry to normal antecedent soil moisture conditions despite high ET demand. There is no evidence that ET has decreased because of cooling. We conclude that the observed increase in late summer groundwater storage and streamflow in the Midwest is caused by the increased July precipitation.

4. Summary and Discussion

[38] In this study, we set out to detect changes in land hydrology in response to the increased July precipitation over the U.S. Midwest attributed to High Plains irrigation in an earlier study [*DeAngelis et al.*, 2010]. Seasonal analysis of hydrologic variables over Illinois suggests that the seasonal cycle of $P - \mathrm{ET}$ is followed by the soil moisture cycle 1 month later, which is followed by the water table and streamflow cycles another month later; thus, it is expected that the increased July P may be detected in August–September groundwater and streamflow. We analyzed 30 year and longer time series of water table depth at 10 wells in Illinois and streamflow at 46 gauges in the Illinois and Ohio river basins. The Mann-Kendall test for trends indicates that groundwater storage and streamflow have increased in August–September since the onset of irrigation in the High Plains, and these trends were determined to be field significant. Examination of soil moisture response to above-normal July P in the postirrigation era suggests that the increased July P due to High Plains irrigation can be sufficient to reach the shallow water table, at least in normal to wet years, hence providing a possible link between increases in July P and groundwater storage and streamflow. The Mann-Kendall test for trends in pan evaporation and atmospheric vapor pressure deficit, both indicators of atmospheric ET demand, suggests that the ET demand has remained constant. The latter points to the soil water availability as the driver in changes in ET and the possibility of increased ET because of the increased P. An annual water balance study by *Teuling et al.* [2009] gives further evidence of increased ET due to increased P. By ruling out the reduction in ET as a cause, we conclude that the observed increase in groundwater storage and streamflow in

Table 7. July Relative Humidity and Temperature Site Information and Mann-Kendall Test Results for Trends in the Atmosphere Vapor Pressure Deficit (VPD) Over 1940–1980[a]

							July Atmosphere VPD			
U.S. Air Force Site	Site Name	State	Latitude	Longitude	Elevation (m)	Period	Mann-Kendall Test Statistic S	Z Statistic	p Value	Trend
725300	Chicago/O'Hare ARPT	Illinois	41.986	−87.914	63	1946–1977	90	1.7583	0.08	increasing
724338	Scott AFB MidAmeric	Illinois	38.545	−89.835	43	1938–1998	−48	−0.5279	0.60	decreasing
725335	Grissom ARB	Indiana	40.650	−86.150	75	1955–1993	67	1.7431	0.08	increasing

[a]No significant trends (at the 5% level) are found at the three sites.

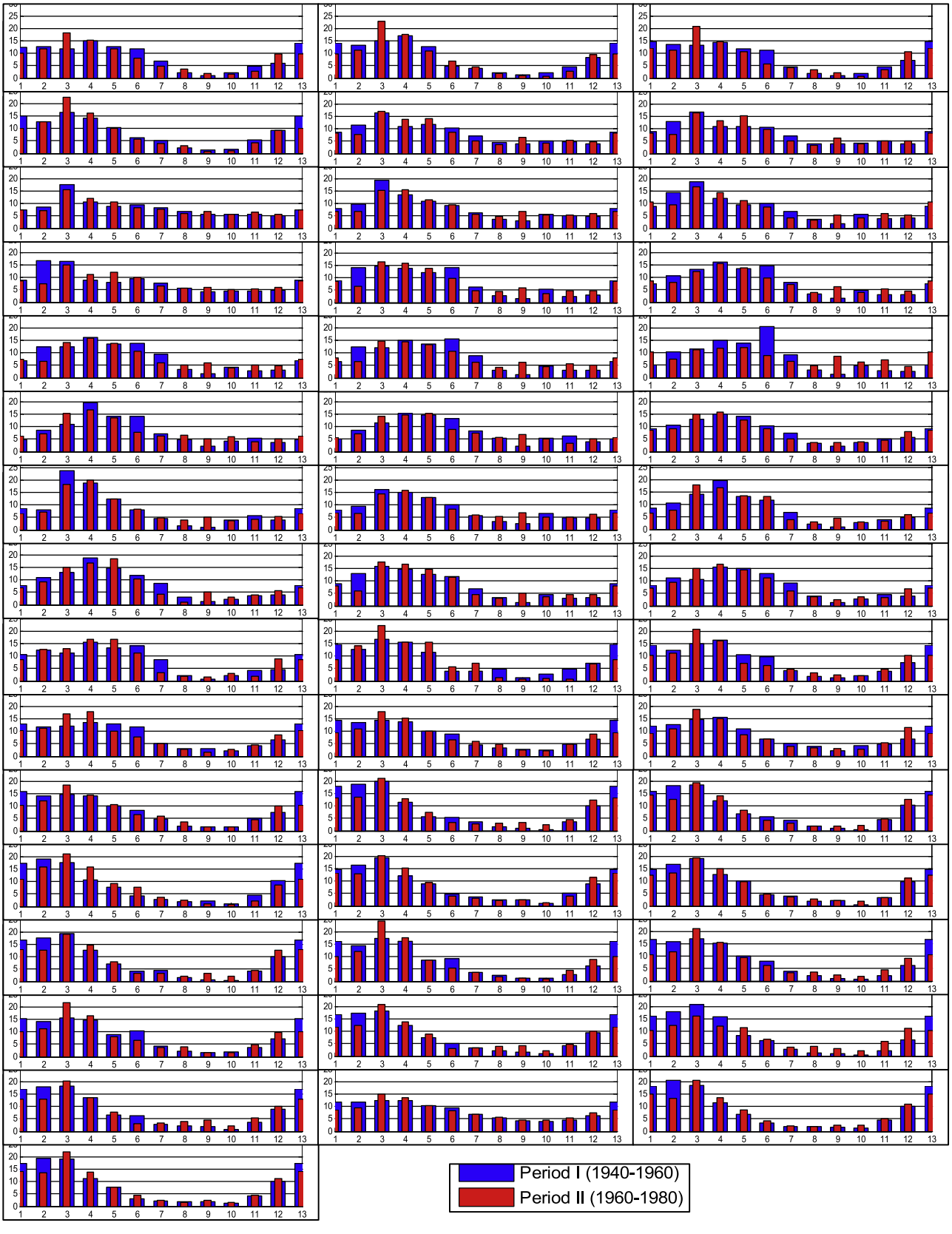

Figure 11. Changes in streamflow seasonal cycle at the 46 gauges (as percent annual total).

the Midwest is linked to the increased July precipitation attributed to High Plains irrigation.

[39] We briefly address the effect of land use change. Historic reconstructions [e.g., *Ramankutty and Foley*, 1999; *Bonan*, 2001] of the Midwestern states suggest accelerated conversion of forest to cropland over 1850–1900, but it has slowed down significantly since then. In addition, forest to cropland conversion has been shown to increase ET [*Bonan*, 1999, 2001; *Baidya Roy*, 2003; *Diffenbaugh*, 2009], not to decrease ET. Urban expansion can also affect water budget, but greater paved area is known to reduce groundwater recharge, not to increase it. Therefore, land use change cannot explain the observed increase in late summer groundwater storage and streamflow.

[40] Last, to place the observed increase in summer streamflow in the context of seasonal dynamics, we plot in Figure 11 the seasonal cycle difference at the 46 gauges between two periods, 1940–1960 (early irrigation development) and 1960–1980 (late irrigation development). Changes in August–September, the focus of this study, are rather small compared to changes in March–April at many gauges; hence, its signal is buried in the total annual flow, which is often the focus of regional hydrologic change studies [e.g., *Groisman et al.*, 2001; *Zhang and Schilling*, 2006; *Qian et al.*, 2007; *Kalra et al.*, 2008; *Raymond et al.*, 2008]. We note that it is important to isolate the signals of change in different seasons because they are likely caused by different mechanisms. Although the signal of summer change is small, it is conceptually significant in that it may point to human modification of the water cycle in the far-away High Plains region as a possible source and cause.

[41] Our results and their interpretations are limited by the available observations, particularly the sparse and short records in water table depths, the lack of soil moisture observations in the preirrigation era, and, particularly, the lack of actual ET measurements. A regional climate-hydrology model simulation over the irrigation development era, similar to the approach by *Puma and Cook* [2010] but with fully integrated hydrologic (including groundwater) and climatic interactions and feedbacks, may help to disentangle the different causes of the observed hydrologic changes in the region.

[42] **Acknowledgments.** Support comes from the U.S. National Science Foundation (NSF-ATM-0450334), U.S. Environmental Protection Agency (EPA-STAR-R-834190), and Rutgers University Academic Excellence Fund (AEF2006-07). We thank Mathieu Gerbush and David Robinson at Rutgers University Climate Lab for assisting us in obtaining climate data from the archive at the National Climate Data Center. We also thank three anonymous reviewers for their thoughtful comments and the editors for their handling of the manuscript.

References

Adegoke, J. O., R. Pielke Sr., and A. M. Carleton (2007), Observational and modeling studies of the impacts of agriculture-related land use change on planetary boundary layer processes in the central U.S., *Agric. For. Meteorol.*, *142*, 203–215, doi:10.1016/j.agrformet.2006.07.013.

Baidya Roy, S., G. C. Hurtt, C. P. Weaver, and S. W. Pacala (2003), Impact of historical land cover change on the July climate of the United States, *J. Geophys. Res.*, *108*(D24), 4793, doi:10.1029/2003JD003565.

Bonan, G. (1999), Frost followed the plow: Impacts of deforestation on the climate of the United States, *Ecol. Appl.*, *9*(4), 1305–1315.

Bonan, G. (2001), Observational evidence for reduction of daily maximum temperature by croplands in the Midwest United States, *J. Clim.*, *14*, 2430–2442.

Boucher, O., G. Myhre, and A. Myhre (2004), Direct human influence of irrigation on atmospheric water vapour and climate, *Clim. Dyn.*, *22*, 597–603, doi:10.1007/s00382-004-0402-4.

Brutsaert, W., and M. B. Parlange (1998), Hydrologic cycle explains the evaporation paradox, *Nature*, *396*, 30.

DeAngelis, A., F. Dominguez, Y. Fan, A. Robock, M. D. Kustu, and D. Robinson (2010), Evidence of enhanced precipitation due to irrigation over the Great Plains of the United States, *J. Geophys. Res.*, *115*, D15115, doi:10.1029/2010JD013892.

Diffenbaugh, N. S. (2009), Influence of modern land cover on the climate of the United States, *Clim. Dyn.*, *33*, 945–958, doi:10.1007/s00382-009-0566-z.

Dominguez, F., J. C. Villegas, and D. D. Breshears (2009), Spatial extent of the North American monsoon: Increased cross-regional linkages via atmospheric pathways, *Geophys. Res. Lett.*, *36*, L07401, doi:10.1029/2008GL037012.

Douglas, E. M., R. M. Vogel, and C. N. Kroll (2000), Trends in floods and low flows in the United States: Impact of spatial correlation, *J. Hydrol.*, *240*, 90–105.

Eltahir, E., and P. J.-F. Yeh (1999), On the asymmetric response of aquifer water level to floods and droughts in Illinois, *Water Resour. Res.*, *35*, 1199–1217, doi:10.1029/1998WR900071.

Feddema, J., K. Oleson, G. Bonan, L. Mearns, W. Washington, G. Meehl, and D. Nychka (2005), A comparison of a GCM response to historical anthropogenic land cover change and model sensitivity to uncertainty in present-day land cover representations, *Clim. Dyn.*, *25*, 581–609, doi:10.1007/s00382-005-0038-z.

Govindasamy, B., P. B. Duffy, and K. Caldeira (2001), Land use changes and Northern Hemisphere cooling, *Geophys. Res. Lett.*, *28*, 291–294, doi:10.1029/2000GL006121.

Groisman, P. Y., R. W. Knight, and T. R. Karl (2001), Heavy precipitation and high streamflow in the contiguous United States: Trends in the twentieth century, *Bull. Am. Meteorol. Soc.*, *82*(2), 219–246.

Haddeland, I., T. Skaugen, and D. P. Lettenmaier (2007), Hydrologic effects of land and water management in North America and Asia: 1700–1992, *Hydrol. Earth Syst. Sci.*, *11*, 1035–1045, doi:10.5194/hessd-3-2899-2006.

Hollinger, S. E., and S. A. Isard (1994), A soil moisture climatology of Illinois, *J. Clim.*, *7*, 822–833.

Kalra, A., T. C. Piechota, R. Davies, and G. A. Tootle (2008), Changes in US streamflow and western US snowpack, *J. Hydrol. Eng.*, *13*, 156–163, doi:10.1061/(ASCE)1084-0699(2008)13:3(156).

Kendall, M. G. (1975), *Rank Correlation Methods*, Charles Griffin, London.

Khaliq, M. N., T. Ouarda, P. Gachon, L. Sushama, and A. St-Hilaire (2009), Identification of hydrological trends in the presence of serial and cross correlations: A review of selected methods and their application to annual flow regimes of Canadian rivers, *J. Hydrol.*, *368*, 117–130, doi:10.1016/j.jhydrol.2009.01.035.

Kueppers, L. M., M. A. Snyder, and L. C. Sloan (2007), Irrigation cooling effect: Regional climate forcing by land use change, *Geophys. Res. Lett.*, *34*, L03703, doi:10.1029/2006GL028679.

Kustu, M. D., Y. Fan, and A. Robock (2010), Large-scale water cycle perturbation from irrigation in the High Plains: A synthesis of observed streamflow changes, *J. Hydrol.*, *390*, 222–244, doi:10.1016/j.jhydrol.2010.06.045.

Lawrimore, J. H., and T. C. Peterson (2000), Pan evaporation trends in dry and humid regions of the United States, *J. Hydrometeorol.*, *1*, 543–546.

Lettenmaier, D. P., E. F. Wood, and J. R. Wallis (1994), Hydro-climatological trends in the continental United States, 1948–88, *J. Clim.*, *7*(4), 586–607.

Liepert, B. G. (2002), Observed reductions of surface solar radiation at sites in the United States and worldwide from 1961 to 1990, *Geophys. Res. Lett.*, *29*(1), 1421, doi:10.1029/2002GL014910.

Livezey, R. E., and W. Y. Chen (1983), Statistical field significance and its determination by Monte Carlo techniques, *Mon. Weather Rev.*, *111*, 46–59.

Lobell, D. B., G. Bala, and P. B. Duffy (2006), Biogeophysical impacts of cropland management changes on climate, *Geophys. Res. Lett.*, *33*, L06708, doi:10.1029/2005GL025492.

Lobell, D. B., C. Bonfils, and J. M. Faurès (2008), The role of irrigation expansion in past and future temperature trends, *Earth Interact.*, *12*, 1–11.

Mann, H. B. (1945), Nonparametric tests against trend, *Econometrica*, *13*, 245–259.

McGuire, V. L. (2009), Water-level changes in the High Plains Aquifer, predevelopment to 2007, 2005–06, and 2006–07, *U.S. Geol. Surv. Sci. Invest. Rep.*, 2009-5019.

McGuire, V. L., M. R. Johnson, R. L. Schieffer, J. S. Stanton, S. K. Sebree, and I. M. Verstraeten (2003), Water in storage and approaches to

groundwater management, High Plains Aquifer, 2000, *U.S. Geol. Surv. Circ.*, *1243*.

Milly, P. C. D., and K. A. Dunne (2001), Trends in evaporation and surface cooling in the Mississippi River basin, *Geophys. Res. Lett.*, *28*(7), 1219–1222, doi:10.1029/2000GL012321.

Puma, M. J., and B. I. Cook (2010), Effects of irrigation on global climate during the 20th century, *J. Geophys. Res.*, *115*, D16120, doi:10.1029/2010JD014122.

Qian, T., A. Dai, and K. E. Trenberth (2007), Hydroclimatic trends in the Mississippi River basin from 1948 to 2004, *J. Clim.*, *20*, 4599–4614, doi:10.1175/JCLI4262.1.

Ramankutty, N., and J. A. Foley (1999), Estimating historical changes in global land cover: Croplands from 1700 to 1992, *Global Biogeochem. Cycles*, *13*, 997–1027, doi:10.1029/1999GB900046.

Raymond, P. A., N. H. Oh, R. E. Turner, and W. Broussard (2008), Anthropogenically enhanced fluxes of water and carbon from the Mississippi River, *Nature*, *451*, 449–452, doi:10.1038/nature06505.

Renard, B., et al. (2008), Regional methods for trend detection: Assessing field significance and regional consistency, *Water Resour. Res.*, *44*, W08419, doi:10.1029/2007WR006268.

Teuling, A. J., et al. (2009), A regional perspective on trends in continental evaporation, *Geophys. Res. Lett.*, *36*, L02404, doi:10.1029/2008GL036584.

van der Ent, R. J., H. H. G. Savenije, B. Schaefli, and S. C. Stelle-Dunne (2010), The origin and fate of atmospheric moisture over continents, *Water Resour. Res.*, *46*, W09525, doi:10.1029/2010WR009127.

van Heerwaarden, C. C., J. Vilà-Guerau de Arellano, and A. J. Teuling (2010), Land-atmosphere coupling explains the link between pan evaporation and actual evaporation trends in a changing climate, *Geophys. Res. Lett.*, *37*, L21401, doi:10.1029/2010GL045374.

Weaver, S. J., S. Schubert, and H. Wang (2009), Warm season variations in the low level circulation and precipitation over the central United States in observations, AMIP simulations, and idealized SST experiments, *J. Clim.*, *22*, 5401–5420, doi:10.1175/2009JCLI2984.1.

Wild, M. (2009), Global dimming and brightening: A review, *J. Geophys. Res.*, *114*, D00D16, doi:10.1029/2008JD011470.

Yang, D. Q., B. S. Ye, and D. L. Kane (2004), Streamflow changes over Siberian Yenisei River Basin, *J. Hydrol.*, *296*, 59–80, doi:10.1016/S0022-1694(04)00182-9.

Yeh, P. J.-F., M. Irizarry, and E. A. B. Eltahir (1998), Hydroclimatology of Illinois: A comparison of monthly evaporation estimates based on atmospheric water balance and soil water balance, *J. Geophys. Res.*, *103*(D16), 19,823–19,837, doi:10.1029/98JD01721.

Yue, S., and C. Y. Wang (2002), Regional streamflow trend detection with consideration of both temporal and spatial correlation, *J. Climatol.*, *22*, 933–946, doi:10.1002/joc.781.

Zhang, Y. K., and K. E. Schilling (2006), Increasing streamflow and baseflow in Mississippi River since the 1940s: Effect of land use change, *J. Hydrol.*, *324*, 412–422, doi:10.1016/j.jhydrol.2005.09.033.

Y. Fan and M. D. Kustu, Department of Earth and Planetary Sciences, Rutgers, State University of New Jersey, Wright-Rieman Labs, 610 Taylor Rd., Piscataway, NJ 08854-8066, USA. (yingfan@rci.rutgers.edu)

M. Rodell, Hydrological Sciences Branch, NASA Goddard Space Flight Center, Greenbelt, MD 20771, USA.